Engineered quasi-phase-matching for laser techniques [Invited]

X. P. Hu,[1,2] P. Xu,[1] and S. N. Zhu[1,*]

[1]*National Laboratory of Solid State Microstructures and School of Physics, Nanjing University, Nanjing 210093, China*
[2]*e-mail: xphu@nju.edu.cn*
**Corresponding author: zhusn@nju.edu.cn*

Received March 18, 2013; revised July 20, 2013; accepted August 8, 2013;
posted September 23, 2013 (Doc. ID 187283); published November 8, 2013

The quasi-phase-matching (QPM) technique has drawn increasing attention due to its promising applications in areas such as nonlinear frequency conversion for generating new laser light sources. In this paper, we will briefly review the main achievements in this field. We give a brief introduction of the invention of QPM theory, followed by the QPM-material fabrication techniques. When combing QPM with the solid-state laser techniques, various laser light sources, such as single-wavelength visible lasers and ultraviolet lasers, red–green–blue three-fundamental-color lasers, optical parametric oscillators in different temporal scales, and passive mode-locking lasers based on cascaded second-order nonlinearity, have been presented. The QPM technique has been extended to quantum optics recently, and prospects for the studies are bright.

OCIS codes: (190.2620) Harmonic generation and mixing; (190.4160) Multiharmonic generation; (160.4330) Nonlinear optical materials; (140.3613) Lasers, upconversion; (140.4050) Mode-locked lasers; (140.7300) Visible lasers.

http://dx.doi.org/10.1364/PRJ.1.000171

1. INTRODUCTION TO QUASI-PHASE-MATCHING

The first laser action was demonstrated in ruby by Maiman in the early 1960s [1]. The high peak power and excellent coherent properties of the laser immediately opened up new research topics, including one of the most important ones, 'nonlinear optics'. In 1961, just one year after the invention of the ruby laser, Franken *et al.* observed second-harmonic generation (SHG) by projection of intense ruby laser light through crystalline quartz [2], which marked the birth of the field of nonlinear optics. By employing nonlinear optical frequency conversions, including sum-frequency generation (SFG), difference-frequency generation, and optical parametric oscillation and amplification, as well as the most well-known SHG, the wavelength of light can be converted to different wavelengths to obtain new laser light sources not readily available. In nonlinear optical interactions, because of the dispersive nature of crystal, the fundamental frequency and the generated frequency travel at different speeds in the material, so there is a phase mismatch between the interacting waves. This phase mismatch will cause the fundamental and the harmonic waves to go out of phase; thus the energy will flow back and forth between them, resulting in a low frequency conversion efficiency. The most common procedure for achieving phase-matching is to use the birefringence of some crystals, which may offset and obtain phase-matching in some wavelength region by choosing the dispersion orientation or the operating temperature of the crystal. This method is the so-called birefringence-phase-matching (BPM) technique, which was proposed by Kleinman in 1962 [3]. In the same year, Armstrong *et al.* [4] suggested a scheme that uses a periodic modulation of the sign of the crystal's quadratic nonlinear coefficient $\chi^{(2)}$ to periodically offset the phase mismatch between the interacting waves by the reciprocal vector of the lattice structure. The proposed method is called the quasi-phase-matching (QPM) technique, and QPM has several advantages over BPM: first, QPM accesses the largest nonlinear coefficient d_{33} because the fundamental and harmonic waves can have the same polarization; second, QPM can avoid the spatial walk-off effect of BPM; third, QPM can be realized for any mixing interaction for which the material is transparent, even in crystals that have too weak birefringence for realizing BPM.

2. MATERIAL FABRICATION

QPM can be realized by periodical inversion of the spontaneous polarization of ferroelectric nonlinear crystal (NLC) materials, and this kind of materials with modulated micrometer-scale domain structures is usually called optical superlattice. As mentioned above, QPM was proposed early in 1962, but could not be experimentally realized at that time because suitable fabrication techniques had not been developed. Early attempts to obtain periodical sign reversal of the second-order nonlinear coefficient were accomplished by utilizing stacked plates of a nonlinear material where adjacent layers are rotated by 180 deg [5–8]. An obvious disadvantage of this method is that multiple Fresnel reflections would introduce additional losses, hence lower the conversion efficiency. In addition, the application of this technique was limited in the far-infrared and terahertz spectral ranges because it is hard to fabricate such plates with thickness down to 100 μm.

In the 1980s, an important breakthrough came when Feng and Ming *et al.* of Nanjing University in China proposed the growth striation technique to obtain $LiNbO_3$ (LN) crystal with

periodic ferroelectric domains in a Czochralski growth system. For this technique, the melt was doped with solute such as yttrium or indium. During crystal growth, a temperature fluctuation was introduced into the solid–liquid interface either by applying a modulated electric current or by an eccentric rotation. And this resulted in periodic solute concentration fluctuation in the crystal along the direction of growth, or the so-called growth striation. The periodic ferroelectric domain can be automatically induced by the growth striations when the growing crystal cools through the Curie temperature [9,10]. By exploiting the growth striation technique, Feng *et al.* prepared LN crystal with periodic laminar ferroelectric domains, and with this crystal, quasi-phase-matched SHG was experimentally verified [11]. Later, a similar procedure was applied to grow $LiTaO_3$ (LT) superlattices [12]. Besides Feng *et al.*'s work, in the 1980s, Fejer and co-workers prepared LN single-crystal fiber using laser-heated pedestal growth [13,14], which was initiated in 1974 at Stanford University. Periodically poled LN (PPLN) single-crystal fibers with micrometer-scale domains were used for the generation of blue [15] and green light [16] by SHG.

Almost at the same time, efforts including chemical diffusion and substitution of impurities were made to control domain inversion at the surface of ferroelectric crystals. In 1989, the group led by Fejer used titanium diffusion followed proton exchange to fabricate an LN waveguide with periodic domain structure, and demonstrated the first quasi-phase-matched green [17] and blue generations [18] in waveguides. Similar results on the LN waveguide were obtained simultaneously by Webjörn *et al.* in Sweden [19] and in Japan [20], as well as the progress in KTP by Bierlein and co-workers [21,22].

Although direct growth of periodical structured NLCs might be adequate for device demonstration, this technique was not so flexible for mass production. In the 1990s, one new method, the lithographic-patterned electric-field poling technique, was developed for creating inverted domains with controlled period and duty cycle at a wafer scale. The significant breakthrough was achieved by Yamada *et al.* of Sony in LN crystal in 1993 [23], following the work by Ito *et al.*, which demonstrated fabrication of LN periodic domain structure by electron-beam poling [24]. Since then, much attention has been paid toward fabricating periodic patterns in thicker LN samples [25] as well as other ferroelectrics, such as LT [26], KTP [27], and SBN [28], using the electric-field poling technique. The processing recipe for electric-field poling is simple. As indicated in Fig. 1, a patterned electrode produced with a photolithographic process was made on the $+z$ surface of the single-domain crystal wafer, while a planar electrode was on the $-z$ surface. High voltage over the coercive field was applied to the plus (+) electrode to reverse the polarization under the patterned electrode; thus the reversed domain was defined by the patterned electrode.

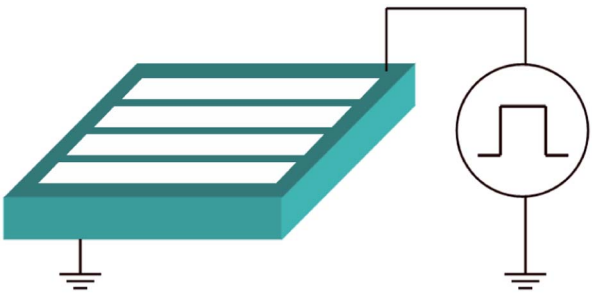

Fig. 1. Schematic setup of the electric-field poling technique.

With the aim of fabricating ferroelectric domain structures with high optical-quality, large-aperture, submicrometer periodicity over large crystal thickness, and with the development of new quasi-phase-matched nonlinear materials, up to now, the electric-field poling technique has been well-developed, and there are several improved methods for better domain control. Myers *et al.* [29] used an electrolyte as a liquid electrode to achieve field uniformity as well as avoid dielectric breakdown during poling LN crystals, and this method was adopted by many research groups. In 1995, 3 in. diameter LN wafers with modulated domain structures were achieved at Stanford University [30]. The extremely high coercive electric fields of congruent $LiNbO_3$ (CLN), which are about 21 kV/mm, and the strong effect of domain widening limit the thickness of the poling crystals to 0.5 mm and the period to be in the range of 10 to 30 μm, which were suitable for infrared (IR) devices. To obtained smaller domain structures for visible light generation, Miller *et al.* [31] obtained PPLN with less than 10 μm periodicity, and later in 1999, a backswitching method was exploited by Batchko *et al.* [32] for fabrication of short-pitched PPLN with 4 μm period and was used for first-order continuous-wave (CW) single-pass 460 nm blue-light generation. An alternative approach for the fabrication of short-period domain in LN single crystals is the surface poling technique proposed by Busacca and co-workers [33,34] at the University of Southampton. This technique is based on conventional electric-field poling, but involves an intentional overpoling step that inverts all the material except a thin surface region directly below the patterned photoresist, and the produced domain period is ~1 μm.

As is known, CLN crystals suffer from optical damage and the photorefraction effect thus limits the applications in high-power laser operations. Research revealed that when doping with 5.0 mol. % MgO, the optical damage threshold can be raised by 2 orders of magnitude [35] and the coercive of MgO-doped LN (MgO:LN) is reduced to be about 1/5 that of CLN [36]. One property of MgO:LN is that it behaves like a diode when the polarization inversion is formed [37]; thus local penetrations would degrade the uniformity of the electric field by the large leakage current of polarization-inverted regions. Sugita *et al.* [38] proposed a multipulse poling method, and this method can suppress current leakage in penetration of the inverted region by using a thick crystal and short-pulse application. Besides, Ishizuki *et al.* [39] reported that the coercive field of MgO:LN crystal was drastically reduced at elevated temperatures. Using the multipulse poling method at elevated temperatures, they succeeded in fabricating 3-mm-thick periodically poled MgO:LN (MgO:PPLN) of 30 μm period with smooth surfaces [40]. Ishizuki and Taira set the record of thickness to be 5 mm for MgO:PPLN in 2005 [41], and 5 mm for MgO-doped periodically poled LT (MgO:PPLT) in 2010 [42]. In 2012, a 10-mm-thick MgO:PPLN was successfully fabricated (see Fig. 2), and was used for construction of a high-energy optical parametric oscillator (OPO) [43]. Another advantage of the multipulse poling method is that it can suppress the side growth of the domain-inverted region, and thus is a promising approach for fabrication of short-period domain structures. By using the multipulse poling method, Sugita and co-workers

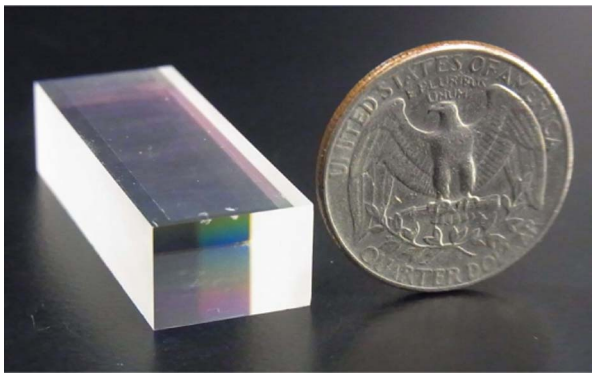

Fig. 2. 10-mm-thick MgO:PPLN with a poling period of 32.2 μm. Selected from Ref. [43].

[38,44] fabricated MgO:PPLN with the periods of 2.2 and 1.4 μm, respectively, and realized efficient first-order ultraviolet (UV) light generations by SHG.

There are also growing interests in light mediated ferroelectric domain engineering of LN single crystal, including light-assisted poling, UV laser-induced inhibition of poling, and all-optical poling methods, also overviewed by Ying *et al.* [45]. Briefly, laser irradiation, from deep-UV to the long-wavelength IR spectral range, can modify the coercive and nucleation field of LN single crystals, and can even induce domain inversion without applying any external electric field. And the light-mediated methods are suitable for fabrication of waveguide nonlinear optical devices, curved domain shapes for photonic applications, and thicker domain-engineered crystals for high peak power nonlinear applications due to the significant reduction of the coercive field.

In addition to LN and LN-family crystals, the poling techniques of KTP are progressing rapidly, and these were mainly accomplished by the Laurell group in Sweden. The demonstration of electric-field poling of hydrothermally grown KTP was realized in 1994 [46]. Later, two improved methods, Rb-exchange-assisted electric-field poling [47] and a low-temperature poling [48], were developed to reduce the ion conductivity of the flux-grown KTP crystals. Due to the large anisotropy of KTP, the domain broadening during electric-field poling is reduced; thus it is favorable for submicrometer-periodic-domain inversion [49]. To further fabricate domain structure with submicrometer periodicity, Canalias *et al.* [50] utilized a chemical patterning method to avoid domain broadening due to the metal electrodes fringing fields. Using this technique, PPKTP crystal with a 720 nm period was fabricated for backward SHG [51], and one with 800 nm period was used to demonstrate experimentally the magic mirror-less optical parametric oscillation [52].

Besides the commonly used QPM materials, LN, LT, and KTP families, techniques for fabricating periodic structures in semiconductors such as GaAs, which is promising for mid-IR, and crystalline quartz, which is suitable for UV generation, are also of interest. For GaAs, epitaxial growth over an orientation-patterned GaAs (OP-GaAs) template was exploited [53]. Meanwhile, for crystalline quartz, the periodic structure can be realized by applying mechanical stress [54].

In the following, we will briefly review some of the solid-state lasers based on QPM materials, including single-wavelength lasers covering red to the UV, red–green–blue (RGB) three-color lasers based on the multiple-QPM technique, OPOs in different temporal scales, and passive mode-locking lasers using cascaded second-order nonlinearity.

3. SINGLE-WAVELENGTH VISIBLE AND UV LASERS USING QUASI-PHASE-MATCHING

Nowadays, laser diodes (LDs) are used in many applications due to their advantages of compactness, high efficiency, good reliability, and low cost. Reliable laser light sources are available in the wavelength range from 630 to 2000 nm. However, many applications require wavelengths outside this wavelength range. For example, blue–green light sources are required in applications such as display, medicine, optical data storage, and color printing. The present blue–green light sources are based mostly on gas lasers or resonant frequency-converted solid-state lasers, which are complex, inefficient, or have a limited wavelength range. Frequency upconversions utilizing QPM optical superlattice offers a way to obtain compact, efficient solid-state laser light sources in the visible and down to the UV spectral range.

A. Red Lasers

Red light can be obtained through the following schemes. The first is direct frequency doubling of the IR lasers at around 1.3 or 1.5 μm. He *et al.* [55] obtained 840 mW red light at 671 nm by single-pass frequency doubling of a Nd:YVO_4 1342 nm IR laser with a PPLT, the SHG efficiency being 60%. Hu *et al.* [56] used a 1.2-mm-thick periodically poled near stoichiometric LT (PPSLT) crystal for frequency doubling and obtained 1.4 W 671 nm red light, with a conversion efficiency of more than 50%. In stoichiometric crystals, the nonstoichiometric defects are significantly reduced, which leads to a reduction of the coercive field by one order; thus samples with thickness more than 1 mm could be easily fabricated with good penetrability; see Fig. 3. In addition, the laser damage threshold of SLT is increased by two or three orders compared with congruent ones. Due to the high optical quality of the PPSLT crystal, the NLC can handle more power, the output power of red was stable, and the output beam exhibited a circular shape with a Gaussian profile as shown in Fig. 4. Hu *et al.* [57] also scaled the output power to 2.4 W at 660 nm, a more bright red light, by using a high-power diode-side-pumped Nd:YAG laser

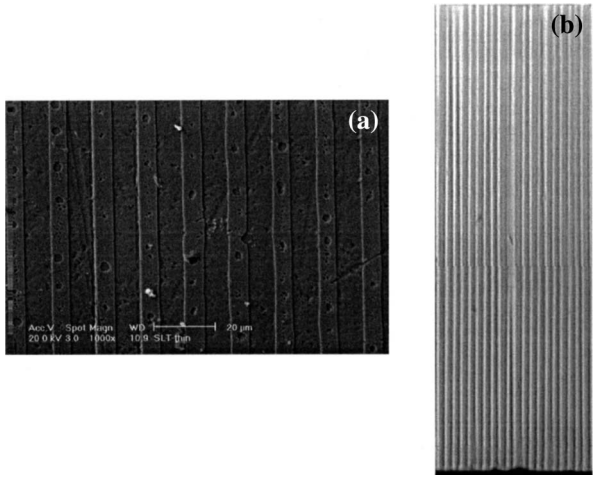

Fig. 3. (a) Scanning electron microscopy micrograph of etched domain-inverted patterns on the +C surface. (b) Cross-section view of Y face of a PPSLT sample. Selected from Ref. [56].

Fig. 4. Output red beam with a Gaussian profile selected from Ref. [56].

operating at 1319 nm as the fundamental source, and the NLC was also a PPSLT but with different poling period. Figure 5 shows the model machine of the high-power 660 nm red laser made at Nanjing University. Thompson *et al.* [58] demonstrated generation of more than 900 mW tunable CW red light at 780 nm by single-pass frequency doubling a seeded fiber amplifier at 1560 nm with two cascaded PPLN crystals. The enhancement of SHG efficiency compared with using one single NLC is due to the presence of second-harmonic (SH) light from the first crystal acting as a seed for the second. Using the cascaded NLC scheme, Chiow *et al.* [59] obtained 43 W quasi-continuous 780 nm red light by single-pass frequency doubling two high-power coherently combined fiber amplifiers at 1560 nm with two cascading PPLN crystals. The total SHG efficiency is up to 66%.

The second scheme is based on frequency mixing of 1.06 and 1.55 μm laser lights. Hart *et al.* [60] and Boullet *et al.* [61], respectively, obtained 630 nm red light by frequency mixing of an Er/Yb-codoped fiber laser operating at 1060 and 1550 nm with a PPLN. Champert *et al.* [62] presented the results on 1.4 W red generation by frequency mixing of seeded Yb and Er fiber amplifiers.

The third scheme for red light generation is by utilizing a direct OPO process in which the frequency of the generated red light is tunable, as indicated by Melkonian *et al.* [63]. They built the first CW oscillation of a single resonant OPO (SRO) operating from 619 to 640 nm with a MgO-doped periodically poled stoichiometric $LiTaO_3$ (MgO:PPSLT) crystal pumped by a 532 nm green laser, and 100 mW of single-frequency red light was obtained.

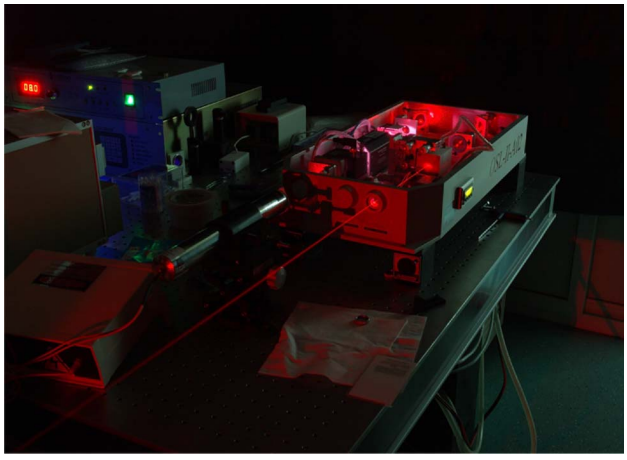

Fig. 5. High-power 660 nm red laser model machine with PPSLT.

The fourth one is based on OPO cascaded SFG. Bosenberg *et al.* [64] reported a 2.5 W CW 629 nm red laser based on a two-step OPO and SFG process carried out in a single PPLN crystal having two periodic gratings in series.

B. Green Lasers

To obtain green light, frequency doubling is the commonly used way and most work is focused on high-power CW green light generation with high efficiency. In 1997, Miller *et al.* [65] first realized 2.7 W CW 532 nm green light generation by single-pass frequency doubling of a Nd:YAG laser with a PPLN crystal, and the power conversion efficiency is up to 42%. To construct a high-power room temperature green laser, MgO:LN is a good candidate. Pavel *et al.* [66] used MgO:PPLN to frequency double a Nd:$GdVO_4$ laser in a single-pass configuration; 1.18 W CW green light was obtained with the conversion efficiency being 16.8%. Yb-doped single-frequency fiber lasers were also used as the fundamental sources for efficient and high-power green light generation due to their high power, high beam quality, and narrow linewidth. Tovstonog *et al.* [67] reported 7 W CW 542 nm green generation at room temperature with 35.4% efficiency in a MgO:PPSLT crystal. Also, Kumar *et al.* [68] obtained 9.64 W CW 532 nm green light using a MgO:PPSLT and 6.2 W output with a PPKTP, both from a Yb-fiber laser at 1064 nm. To further improve the efficiency of green light generation, Ricciardi *et al.* [69] placed the PPLT crystal in a resonant enhanced cavity; 6.1 W green light was obtained with a conversion efficiency of 76%, which is the highest ever reported. In addition, Kumar *et al.* [70] used a novel cascaded multicrystal scheme [71] for efficient CW single-pass SHG, which provided more than 55% conversion efficiency. The multicrystal SHG scheme is shown in Fig. 6.

C. Blue Lasers

As for blue-light generation, there are several schemes. Frequency doubling or tripling of the near-IR light is the most commonly used approach. The challenge for first-order quasi-phase-matched frequency doubling or tripling to obtain blue light is the rather small domain period, which is below 5 μm. Pruneri *et al.* [72] fabricated a PPLN crystal with 4.6 μm period by choosing optimized mark-to-space ratio during electric-field poling, and obtained 49 mW CW 473 nm blue light by frequency doubling with a 4.6% conversion efficiency. Batchko *et al.* [73] reported single-pass CW first-order QPM SHG of 60 mW blue light at 465 nm in a backswitched poled PPLN crystal with 4 μm periodicity. Due to the rather low coercive field, which is about 2 kV/mm, stoichiometric $LiTaO_3$ crystal is an alternative for small period (4.6 μm) sample fabrication, and can be used for frequency tripling to obtain blue light at

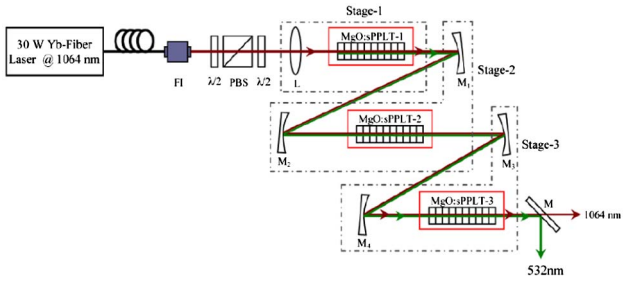

Fig. 6. Schematic experimental setup for the multicrystal CW single-pass SHG. Selected from Ref. [70].

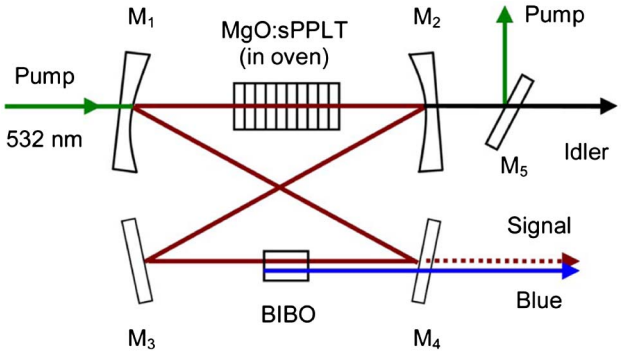

Fig. 7. Schematic of an intracavity frequency-doubled MgO:PPSLT CW SRO for blue generation. Selected from Ref. [77].

440 nm [74]. As for KTP, the low-temperature poling technique was exploited for creation of domain period down to 5 μm for efficient single-pass SHG of 460 nm blue light [75].

Another approach is based on 532 nm green laser pumped OPO cascaded with a SHG or SFG process. This approach was first realized by Xu *et al.* [76] for blue-light generation with 20 nm tuning range in a quasi-periodic LT superlattice. Later, Samanta *et al.* [77] constructed a ring OPO cavity, as shown in Fig. 7, which comprised a MgO:PPSLT crystal placed between two concave mirrors and a BBO crystal placed between plane mirrors. Temperature tuning of MgO:PPSLT together with angular tuning of BBO produced a CW single-frequency blue laser source tunable in the wavelength range of 425–489 nm, and the output power of blue ranged from 45 to 448 mW. Lai *et al.* [78] made a special design, to realize 435 nm blue light through OPO and SHG in a single PPLT crystal. In addition, a tunable blue light can be obtained by intracavity frequency doubling in an external resonator geometry with spatial separation of the spectral components using a fan-structured PPLT crystal [79].

D. 589 nm Yellow Lasers

Laser light sources at 589 nm are of important applications in medicine, communication, display technology, and sodium guide stars. There are mainly two ways to generate 589 nm yellow light: the first one is based on frequency mixing of the two emission lines of the Nd:YAG laser gain media, which are 1064 and 1319 nm, respectively, and the second one is by direct frequency doubling of a Raman fiber amplifier laser. For the first scheme, two IR lasers can be used with different NLCs such as LN [80], PPLN [81], PPSLT [82], and PPKTP [83], and a high average power of more than 16 W was obtained, though the laser system is complex. To make the system more compact, Zhao *et al.* [84] used a Nd:YAG dual-wavelength laser as the fundamental source and a PPLT crystal as the nonlinear frequency converter, as shown in Fig. 8. The three-mirror laser cavity, which was proposed by Chen

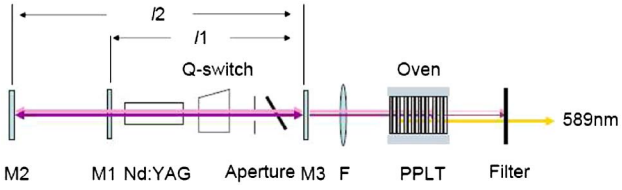

Fig. 8. Schematic setup for 589 nm yellow generation by frequency mixing a dual-wavelength IR laser. Selected from Ref. [84].

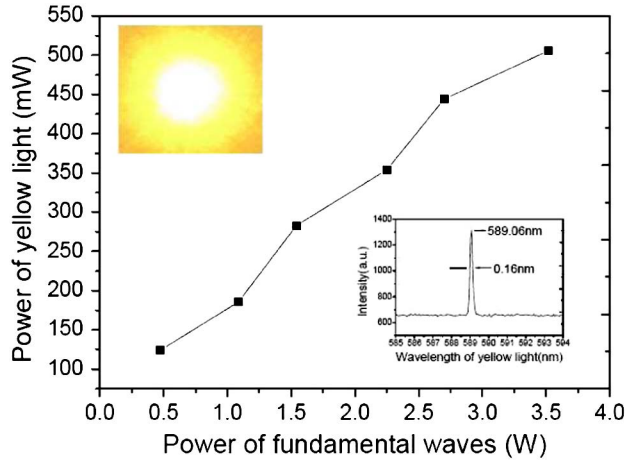

Fig. 9. Power dependence of the output yellow light on the total pumping power in [84]. The inset on the top left is a picture of the output yellow beam, and the insert on the bottom right is the spectrum of 589 nm yellow light.

and co-workers [85,86], can be used to adjust the power ratio between the two emission lines for efficient SFG and can improve the stability of the dual-wavelength laser system as well. By single-pass SFG, 500 mW 589 nm yellow with a 0.16 nm spectral width was obtained, as indicated in Fig. 9.

Direct frequency doubling of a Raman fiber amplifier is an alternative approach for high-power narrow-linewidth CW 589 nm yellow light generation. Georgiev *et al.* [87] obtained 3 W CW 589 nm yellow light by frequency doubling a 1179 nm Raman laser using a MgO:PPLN crystal. Yuan *et al.* [88] also reported 4 W CW 589 nm laser from a Raman fiber amplifier with a MgO:PPSLT as the frequency-doubling crystal. Figure 10 shows the spectrum of the frequency-doubled 589 nm yellow light, the FWHM being about 0.2 pm, which is suitable for the sodium guide star application.

E. UV and Vacuum UV Lasers

Ferroelectric crystals such as LN [89,90], LT [91–94], and KTP [95–97] can be periodically poled for efficient UV generation. But the intrinsic band edge around 300 nm prevents the wavelength conversion to vacuum UV (VUV).

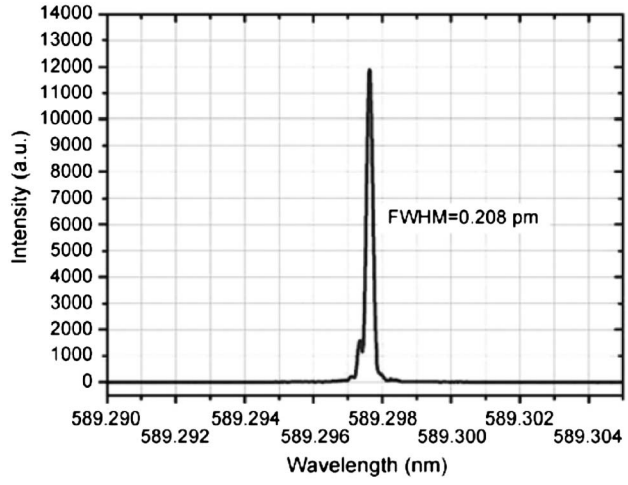

Fig. 10. Spectrum of the 589 nm yellow light by frequency doubling a high-power Raman fiber amplifier. Selected from Ref. [88].

Crystal quartz, however, has a short UV band edge down to 150 nm, which is suitable for VUV generation. Recently, Kurimura *et al.* [54] created periodically twinned crystal quartz with modulated polarity by applying mechanical stress, and demonstrated QPM SHG emitting VUV light at 193 nm.

Besides crystal quartz, the ferroelectric fluoride $BaMgF_4$ shows a very wide transparency range extending from 125 nm to 13 μm, and by using periodical poling, QPM can be achieved in the whole transparent wavelength region [98]. To date, the shortest period obtained is 6.6 μm, which can be used for second-order SHG of 193 nm supposing a suitable duty cycle of the periodically poled crystal.

4. RED–GREEN–BLUE LASERS BASED ON MULTIPLE QUASI-PHASE-MATCHING

Besides single-wavelength solid-state visible and UV lasers, multiwavelength solid-state lasers are also of great interest, such as RGB three-elementary-color lasers. As we all know, all the vivid beautiful colors of the visible world can be constituted through a weighted combination of only three fundamental colors: red, green, and blue. Laser-based projection display (LBPD) has some obvious advantages over the conventional display technique, such as high brightness, high spatial resolution, and great color gamut. One possible way is using three lasers, each emitting light with the wanted color. To date, many attempts for generation of RGB light have been made, and there are mainly two routes: the first one is based on frequency upconversion in series, such as SHG or/and SFG of the pump wavelengths or oscillating wavelengths, and the second approach is based on frequency downconversion cascaded with several frequency upconversion processes.

A. Multiple-QPM Technique

It is obvious that there always involves several nonlinear optical processes for RGB three-color generation, and in this subsection, we will introduce the multiple-QPM technique, which is favorable for compact and efficient RGB laser generation.

In the early years of QPM, research was focused on nonlinear materials with periodic modulated domain structure. As is known, the reciprocal vector of a one-dimensional (1D) periodic optical superlattice can be written as $G_m = m \cdot 2\pi/\Lambda$, where Λ is the grating period and m is the QPM order. And one can see that a periodic optical superlattice provides a series of reciprocal vectors, each of which is an integer times a primitive vector. Hence the reciprocal vectors are independent, and are usually used to efficiently realize one single nonlinear optical parametric process. In 1986, just two years after the invention of quasi-crystal [99], researchers at Nanjing University in China introduced quasi-periodic structure into optical superlattice design, and extended the study of QPM from periodic to quasi-periodic structure. In 1990, Feng *et al.* [100] established the multiple-QPM theory. Later on, various structures, such as aperiodic [101,102], dual-periodic [94,103], as well as two-dimensional (2D) optical superlattice [104–106], were proposed for multiple QPM.

Actually, a 1D quasi-periodic lattice can be created by the projection of 2D square lattice on a straight line [107]. The projection points on the straight line form two types of intervals, a and b. The arranged sequence of a and b depends on the projection angle θ. By analogy, a two-component quasi-periodic optical superlattice is constructed from two building blocks A and B with the widths D_A and D_B, respectively. Both A and B contain a pair of 180 deg antiparallel domains. Assume that all A and B blocks have the same width of positive domains, represented with l. According to the projection theory, the reciprocal vectors for this quasi-periodic structure are $G_{m,n} = 2\pi(m + n\tau)/D$, where $D = \tau D_A + D_B$ is the average structure parameter, m and n are two integers, and $\tau = \tan\theta$. Since θ is an adjustable parameter, it offers the quasi-periodic structure additional design flexibility for QPM. Compared with a 1D periodic structure, a 1D quasi-periodic optical superlattice has a higher symmetry, and its reciprocal vectors are governed two integers m and n; thus some coupled optical parametric processes can be realized. For example, the QPM conditions for third-harmonic generation (THG) via cascaded quadratic nonlinearity are $\Delta k_1 = k_2 - 2k_1 - G_{m,n} = 0$ for SHG and $\Delta k_2 = k_3 - k_2 - k_1 - G_{p,q} = 0$ for SFG, where k_1, k_2, and k_3 are the wave vectors of the fundamental, the SH wave, and the third-harmonic wave, respectively; m, n, p, and q are integers representing the QPM order. In 1997, Zhu *et al.* [108] experimentally demonstrated direct THG in a quasi-periodic optical superlattice with the well-known Fibonacci sequence, of which the structure parameter τ is near the golden ratio, and the THG efficiency was up to 23%. And this pioneering work exhibited a possible important application of quasi-periodic superlattice in nonlinear optics.

B. RGB Laser Based On Frequency Upconversions

In this scheme, the fundamental light sources could be single-wavelength or a multiwavelength ones, and by SHG and/or SFG of the fundamental light, RGB lights can be obtained. Yamamoto *et al.* [109] utilized two LDs, respectively, operating at 1.3 and 0.86 μm as the fundamental sources; simultaneous generation of blue at 0.43 μm, green at 0.52 μm, and red at 0.65 μm by SHG and SFG in a proton-exchanged MgO:LN waveguide was demonstrated for the first time. In 1993, Laurell *et al.* [110] used two IR lasers as the pump light, and by combinations of SHG and SFG in a segmented KTP waveguide, simultaneous generation of UV, blue, and green light was obtained, and this may be the first published QPM multicolor generation. Not long after, Sundheimer *et al.* [111] reported RGB generation through simultaneous SHG, SFG, and fourth-harmonic generation of a single laser source at 1650 nm in a segmented KTP channel waveguide. Following the same idea, Baldi *et al.* [112] realized RGB three-color generation with a proton-exchanged PPLN channel waveguide. Rare-earth-doped LN crystal with modulated domain structure can also be used for simultaneous RGB generation with broad tunability. Cantelar *et al.* [113] fabricated a Zn-diffused Er^{3+}/Yb^{3+}-codoped aperiodically poled LN (aPPLN) channel waveguide. Red light ranging from 650 to 690 nm and green light from 520 to 575 nm arose from energy transfer upconversion processes between the two rare-earth ions, while the blue is produced by QPM SHG of the pump laser.

The above-mentioned RGB light sources were realized in waveguides; as for the bulk, Jaque *et al.* [114] experimentally demonstrated RGB laser generation from a $Nd:YAl_3(BO_3)_4$ employing two different pump wavelengths at 807 and 755 nm. Red at 669 nm was obtained by self-frequency-doubling of the laser oscillation at 1338 nm; the green at 505 nm and the blue at 481 nm were obtained by self-SFG of the fundamental and

the two pump wavelength, respectively. And the need for a two-pump-source is the disadvantage of this scheme. Romero *et al.* [115] realized simultaneous CW RGB generation using a 0.88 μm pumped Nd:YVO_4 1.34 μm laser with a SBN crystal as the intracavity frequency converter. Red and blue light were generated by SHG of the pump and the IR, respectively, while green light was produced by frequency mixing of the pump and IR laser radiation. Due to the broad distribution of ferroelectric domain sizes of SBN, no angle or thermal tuning is need for both SHG and SFG processes.

To realize simultaneous generation of RGB with compactness and efficiency, a promising approach combining the multiwavelength oscillating solid-state laser technique together with the multiple-QPM-theory-based optical superlattice has been developed recently. The Nd^{3+} ion is a very versatile laser active ion and has multiple allowed transitions leading to potential laser radiations around 1300, 1060, and 940 nm, respectively. If these three channels could be oscillated at the same time, simultaneous RGB generation could be implemented by the frequency-doubling technique. However, the line around 940 nm, which belongs to a quasi-three-energy-level system, is too difficult to oscillate due to its rather low gain. In addition, the existing gain competition among these three emission lines makes it almost impossible to oscillate three of them simultaneously. However, there is another possible way that employs frequency tripling of the line around 1300 nm to obtain blue light. With this method, only two fundamental waves around 1300 and 1060 nm are needed for simultaneous RGB generation. In general, there are three nonlinear processes during RGB generation; to make the system more compact, a special NLC is needed and optical superlattice based on multiple-QPM theory may be a good candidate. Capmany [116] realized 1084 and 1372 nm dual-wavelength operation in Nd^{3+}-doped aPPLN, and through frequency doubling of the two IR lights, 542 nm green and 686 nm red were obtained, while frequency mixing of the 744 nm pumping light with the 1084 nm IR produced 482 nm blue. In 2003, He *et al.* [117] and Liao *et al.* [118], both at Nanjing University in China, using a dual-wavelength *Q*-switched Nd:YVO_4 laser operating at 1064 and 1342 nm as the fundamental source, and aperiodically poled LT (aPPLT) crystals as the nonlinear frequency converter, experimentally realized red, yellow, and green "traffic signal lights," as well as RGB three-fundamental-color light. To combine RGB in a proper proportion for white-light generation, Li *et al.* [119] utilized a Nd:YVO_4 dual-wavelength laser and a dual-periodic LT optical superlattice for simultaneous RGB generation, and by changing the pump power and the operating temperature of the optical superlattice, the proportion of RGB was changed as well, and an average quasi-white-light laser power of 530 mW was achieved. In 2008, Hu *et al.* [120] realized 1 W quasi-white-light generation from an intermittent oscillating dual-wavelength Nd:YAG laser operating at 1064 and 1319 nm with a cascaded LT superlattice. The intermittent oscillating scheme composed of a Y-shaped laser cavity with two arms shared the same gain medium and the same output coupling mirror, but had two individual *Q*-switches with a delay between their opening time, thus avoiding the gain competition between the emission lines. (Please refer to Ref. [121] for a detailed description of the intermittent oscillation dual-wavelength laser technique). Another advantage of the

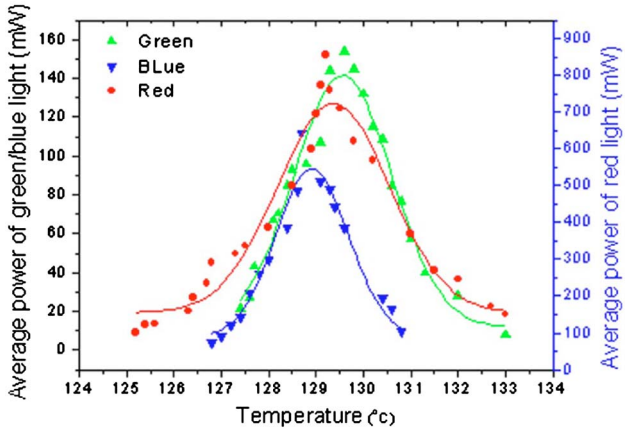

Fig. 11. Temperature tuning curves of the red, green, and blue colors in Ref. [120].

intermittent oscillation dual-wavelength laser technique is that the power proportion of the two oscillating lines is adjustable, so that the power ratio of the RGB three fundamental colors is adjustable to obtain white light. Changing the crystal temperature can also adjust the power ratio of the output RGB beams. The temperature tuning curves of their scheme in Fig. 11 show that red, green, and blue reached the maximum output power at different temperatures, but the temperature tuning curves overlapped each other in a temperature region to ensure simultaneous RGB output. At 129.3°C, 780 mW red light, 146 mW green light, and 84 mW blue light were obtained, the power proportion of RGB being 9.3 : 1.7 : 1, which mixed up into 1.01 W cool white light according to the C.I.E. chromaticity diagram. The conversion efficiency from the power of the two IR beams to the power of the quasi-white light was 20%, and the output power fluctuation was measured to be ~6.5% within 1 h. Figure 12 shows a photo of the RGB beams separated by a prism from the setup.

C. RGB Laser Based On Frequency Downconversions

The dual-wavelength scheme described above for realizing RGB or quasi-white-light output involves a complex arrangement of optical components. They are thus relatively inefficient and are quite expensive to implement in commercial systems. Another scheme for realizing a monolithic RGB laser light source is based on frequency downconversion cascaded with some frequency upconversions.

Henrich *et al.* at University Kaiserslautern [122] developed a 19 W RGB solid-state laser source that is well suited for large frame laser projection displays, and they have brought it all

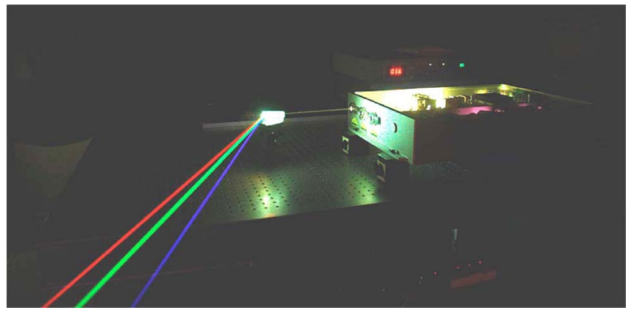

Fig. 12. Photo of the RGB beams separated by a prism from the setup. Selected from Ref. [120].

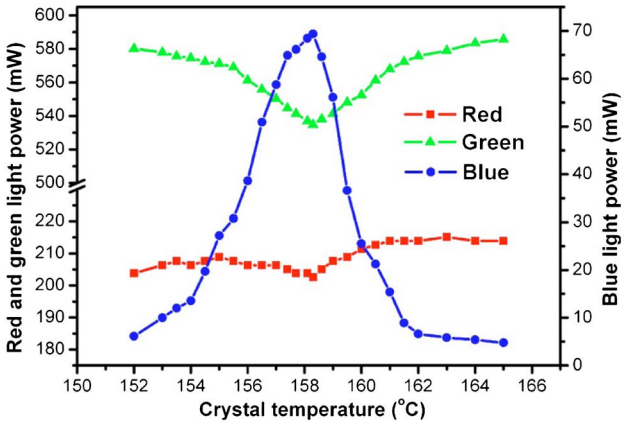

Fig. 13. Temperature tuning curves of the RGB three colors selected from [124].

the way to commercialization. The pumping source used is a high-power mode-locked Nd:YVO_4 1064 nm laser. A KTA-OPO was synchronously pumped to generate a signal wave at 1535 nm and a mid-IR idler wave at 3470 nm. Frequency doubling of the IR laser generates 532 nm green. 629 nm red light results from single-pass sum-frequency mixing of the 1535 nm OPO signal wave and 1064 nm laser radiation in a KTA crystal. Another single-pass SFG process mixes the red light with residual OPO signal radiation to create a 446 nm blue beam. In 2001, Liu *et al.* [123] used a LT crystal with two periodic structure arranged in tandem pumped by a 532 nm green laser to produce red and blue light. Red light at 631 nm was generated as the signal wave by parametric downconversion of the incident green beam. Blue light at 460 nm was obtained by frequency mixing of the residual green light with the mid-IR idler of the former parametric process. Together with the residual green light, three fundamental colors were obtained. Following the same scheme, Gao *et al.* [124] created a monolithic RGB source with a tandem-structured SLT crystal wafer pumped by 1 W high-repetition-rate nanosecond 532 nm green light. Figure 13 gives the temperature tuning curves of RGB three colors at full pumping power of 1 W. At 158.3°C, 69.4 mW blue light was generated, which was the least of the three colors. By blocking the excess red and green powers, 304 mW of color-balanced white light, which included 140 mW red, 94.3 mW green, and 69.4 mW blue, was obtained. The optical-to-optical efficiency from the pump green to the white light was 30%. The generated white light separated with a prism is shown in Fig. 14. By raising the green pump power to 3.7 W, Xu *et al.* [125] scaled the output power of the white light to 1 W with a PPLT crystal.

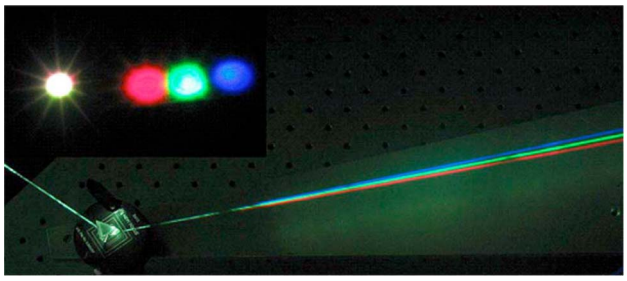

Fig. 14. Generated white light disperses into RGB three colors through a prism. Selected from Ref. [124].

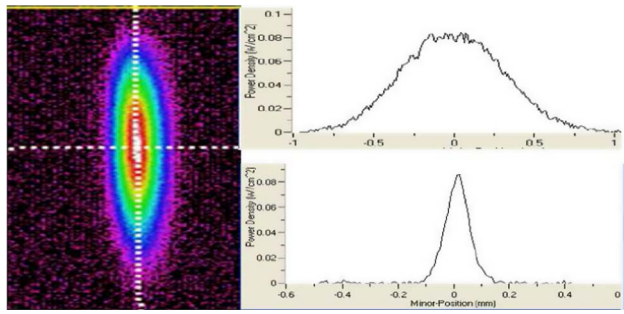

Fig. 15. Elliptical spot at the focus plane of the pump. Selected from Ref. [125].

A unique choice in their work is that a cylindrical lens was used to shape the pump laser into an oblate spot so as to match the shape of the superlattice, as shown in Fig. 15. Besides the pulsed (picosecond and nanosecond time range) RGB laser light sources described above, Lin *et al.* [126] reported a CW watt-level RGB laser pumped by a Yb-fiber laser at 1064 nm. The red, green, and blue lights were obtained by frequency mixing of the pump and the signal wave, frequency doubling the pump IR light, and SFG of the red and the signal wave.

There are also several variants of the green light pumped parametric downconversion RGB source. Cudney *et al.* [127] presented a RGB source based on simultaneous QPM SHG and THG in a single LN crystal wafer with two periodic structure in tandem. In the first part, 1.43 μm signal was generated through optical parametric generation (OPG), and in the second section, SHG and THG of the signal wave produced the red and blue light. Green light was obtained by a nonphase-matched SFG between the signal and the pump wave.

Besides collinear RGB laser light sources from 1D optical superlattice, Xu *et al.* [128] and Zhao *et al.* [129] have demonstrated noncollinear RGB laser light sources from a 2D optical superlattice. The pump sources in both works are 532 nm green lasers; red and blue lights result from a green light pumped OPG process cascading two SHGs of the signal and idler waves in a single-pass setup. The NLCs are a hexagonally poled LT and a 2D nonlinear photonic quasi-crystal, respectively. Owing to the noncollinear reciprocal vectors provided by the 2D optical superlattice, the RGB light was autoseparated without using any optical separation elements, as indicated in Fig. 16.

5. QUASI-PHASE-MATCHED OPTICAL PARAMETRIC OSCILLATORS

Nonlinear optical processes have different forms, and the most important ones include SHG, SFG, difference-frequency generation, and OPG. To extend the spectral range of the emitting light, OPG is of great interest. However, to realize a parametric process for practical use, the NLC is often placed into an optical resonator, and this is the well-known OPO. OPOs are versatile sources of coherent radiation; in particular, combined with QPM materials, they could provide optical radiation across an entire spectral range and over all the temporal scales.

In 1995, Myers *et al.* [130] demonstrated the first bulk QPM OPO, which was almost at the same time as the first QPM

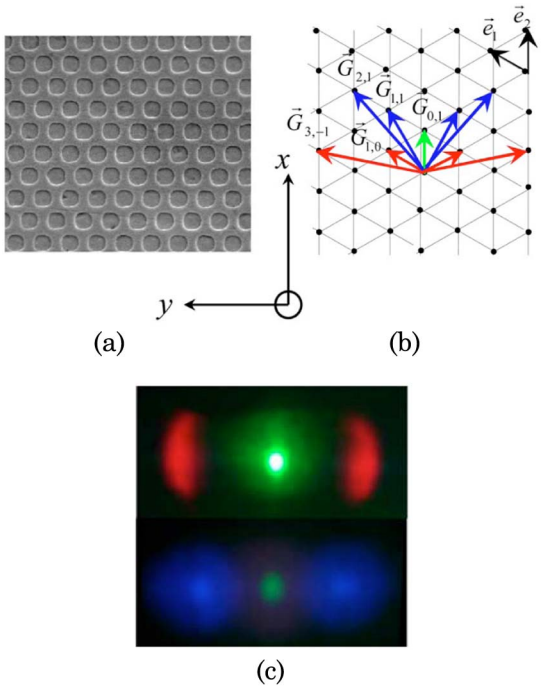

Fig. 16. (a) Micrograph of the HexPLT sample, (b) reciprocal space of the sample, and (c) photograph of the noncollinear RGB colors from the HexPLT. Selected from Ref. [128].

waveguide OPO realized by Bortz *et al.* [131]. The pumping source was a 1.064 μm *Q*-switched Nd:YAG laser, and the output was temperature tuned over the 1.66–2.95 μm spectral range. The NLC was fabricated using the electric-field poling technique with a thickness of 0.5 mm and an interaction length of 5.2 mm. The threshold was about 0.1 mJ, which was more than 1 order of magnitude below the crystal damage limit. For the nanosecond OPOs, the high energy of the pump pulse would demand on the material damage threshold. With the development of QPM materials and material fabrication techniques, optical superlattice with high damage threshold, large aperture, long interaction length, and large effective nonlinearity, together with the advances in pump-laser technology, could cause the output of nanosecond OPOs to produce more and more output. Ishizuki and Taira [42] reported a high-energy OPO of 118 mJ output in 10 ns pulse duration of 30 Hz repetition rate using a 5-mm-thick 39-mm-long MgO:PPLT with a poling period of 30 μm, the slope efficiency being about 70%. They also fabricated a 10-mm-thick Mg:PPLN for handling more energy. In the same 10 ns and 30 Hz pulse region, the output energy reached half-joule (540 mJ) with a total conversion efficiency of more than 76% [43]. Besides, Zukauskas *et al.* [132] demonstrated a high-energy OPO pumped at 1064 nm with 12 ns pulses at 100 Hz repetition rate, using a 5-mm-thick PPKTP with homogeneous and high-quality domain gratings as the NLC. This OPO generated 60 mJ total energy with a 50% conversion efficiency at room temperature.

Ultrafast OPOs, using picosecond or femtosecond pulses as the pump, have also been developed since the 1990s. Pruneri *et al.* [133] reported a SRO in a PPLN crystal synchronously pumped with a 523.5 nm picosecond laser, producing 200 mW average power within the 10 μs envelope, and with a tuning range from 883 to 1285 nm. Almost at the same period, Galvanauskas *et al.* [134] demonstrated the first femtosecond QPM OPO in a PPLN crystal pumped at 777 nm. The output produced 300 fs pulses with a tuning range from 1 to 3 μm. In the ultrafast OPOs, a technique named "synchronous pumping" is necessary for amplification of the generated waves. In this technique, the interval between the arrival of adjacent pump pulses is arranged to match the round-trip time of the frequency downconverted pulse in the OPO cavity, so that the interacting pulses always meet in the NLC. Due to the extremely short pulse duration of the ultrafast pumping pulses, the input optical intensity is high for efficient frequency conversion. In addition, the energy content is rather small (typically from several tens of nanojoules to several hundreds of nanojoules); therefore, the material damage threshold is alleviated. For the QPM ultrafast synchronously pumped OPO, Nd-doped mode-locking lasers, Ti:sapphire lasers, and Yb-doped fiber lasers are commonly used as the pumping sources. Together with the QPM materials, such as PPLN and PPKTP, the ultrafast OPOs can provide pulses across the 1 to 5 μm spectral range from near-IR to mid-IR [135–140].

OPOs in the CW region are a big challenge because the low pump intensity and the subsequent low parametric gain prevent them from being practical. In CW OPOs, at least one of the generated waves should resonante in the cavity to overcome the round-trip loss. Among the different resonating configurations, the SRO is the simplest, with only one signal wave oscillating in the cavity. Compared with double resonant OPO (DRO), SRO does not suffer the stability problem, though the oscillation threshold may be 2 orders of magnitude that of DRO, hence requiring the QPM materials to have suitable interaction lengths and low losses. The first QPM CW SRO operation was reported by Myers *et al.* [141] in a 50-mm-long PPLN crystal with a threshold of 3 W. To get efficient and stable output, the pump power should be several times the oscillation threshold, and this can done by utilizing high-power single-frequency pumping sources [142], reducing the threshold by choosing a suitable interaction length [143], or using high-power broadband lasers as the pumps [144]. To extend the output spectral region to shorter wavelengths, especially in the visible, one can exploit frequency-doubled green laser as the pump to obtain red or yellow light, as well as cascading a SHG/SFG process to get blue light [77,145,146]. One of the challenges of the nonlinear materials used in CW OPO operation is the light absorption, and weak absorption losses will raise the pump threshold to several tens of watts. In addition, light absorption will cause refractive index change through thermal-optical or bulk photorefractive effect. To date, optical cleaning [147] or doping with MgO in LN-family crystals have turned out to be effective methods.

6. PASSIVE MODE-LOCKING LASERS USING OPTICAL SUPERLATTICE

In addition to high-power efficient single-wavelength lasers and RGB three-fundamental-color lasers through QPM, optical superlattice can be used to realize solid-state mode-locking picosecond lasers. There are two mechanisms to achieve passive mode-locking solid-state lasers in the picosecond regime. The first one is nonlinear mirror mode-locking (NLM), which was first proposed by Stankov and Jethwa in 1988 [148]. The NLM scheme consists of a NLC for SHG, a dielectric dichroic mirror having partial reflection at the fundamental and total

reflection at the SH wave, and a dispersive medium between the NLC and the dichroic mirror. The SH generated is completely reflected by the dichroic mirror, and if the SH wave experiences a proper phase shift with respect to the fundamental wave, it can be totally reconverted into a fundamental wave on its way back through the NLC. Hence, the reflectivity of the combination, a frequency-doubling crystal and a dielectric mirror, is intensity dependent. The NLM scheme is simple for picosecond pulse generation, but the longer duration of the output pulse in comparison with the pulse traveling inside the laser cavity is the main drawback. The second mode-locking mechanism, which was first demonstrated by Cerullo *et al.* [149], is called cascaded second-order nonlinear mode-locking (CSM) or cascaded Kerr lens mode locking. The cavity configuration of CSM is essentially the one of NLM, but the dichroic mirror totally reflects both the fundamental wave and the SH wave. The frequency-doubling crystal is placed in off phase-matched condition; thus a nonlinear phase shift will be imprinted on the fundamental wave beam, resulting in nonlinear mode size variations, which can be converted into nonlinear loss modulations together with a suitably positioned intracavity hard or soft aperture. The modulation depth of this scheme will depend on the cavity design and it can be large even for small conversion efficiencies, so it does not exhibit the pulse duration limitation characteristic for NLM.

The nonlinear frequency-doubling crystal used for mode locking can be either BPM material, such as KTP, BBO, and LBO, or QPM material. There are several advantages when using QPM materials as the frequency doubler, as in the following: first, this approach is promising for scaling the power because the damage threshold of NLCs is an order of magnitude higher than that of SESAM and the low residual absorption at the fundamental wave enables operation at high average power; second, due to using QPM, mode locking can work at any wavelength in the NLC's transparent spectral region, so this technique is feasible in wide spectral regions, especially operating at wavelengths where no SESAMs exist. In 2002, Chen *et al.* [150] demonstrated, for the first time, 5.6 W and 20 ps nonlinear mirror mode-locked Nd:YVO_4 laser with a PPKTP; the long pulse duration was mainly due to the group velocity mismatch between the fundamental and the SH waves in the NLM scheme. The schematic experimental setup for diode-pumped passively mode-locking lasers is shown in Fig. 17. A four-mirror laser cavity configuration is usually used to ensure proper mode size in both the laser gain medium and the NLC. The nonlinear frequency-doubling crystals in the schematic are indicated as PPXX. As mentioned above, CSM scheme does not exhibit the pulse duration limitation characteristic compared with NLM. Holmgren *et al.* [151] demonstrated a Nd:$GdVO_4$ laser mode locked by a self-defocusing cascaded Kerr lens in PPKTP; the repetition rate was 200 MHz with an average power of 350 mW. A strong pulse shortening mechanism is produced by the interplay of group velocity mismatch and the cavity design, which leads to a pulse duration as short as 2.8 ps and with a bandwidth of 0.6 nm. Iliev *et al.* [152] utilized similar scheme, achieving stable and self-starting mode locking of a diode-pumped Nd:$GdVO_4$ by employing CSM in a MgO:PPSLT crystal; the maximum average output power reached 5 W and the shortest pulses were 3.2 ps. Besides the results relying on NLM or CSM alone, some hybrid mode-locking techniques have also been reported. In [153], Holmgren *et al.* reported on a Nd:YVO_4 laser mode locking with a hybrid active and passive modulator consisting of a single partially poled KTP crystal. The active phase modulation is done by the electro-optic effect of the unpoled region of the NLC, which initiates, enhances, and stabilizes the mode locking. The periodically poled part provides passive modulation by CSM, which is responsible for pulse shortening. The advantage of this hybrid scheme is that it has short pulses attributed to passive mode locking, but with the active modulation the requirements for self-starting the passive mode locking can be relaxed. By this means, the repetition rate of the laser was 94 MHz and the average output power was 350 mW, with the pulse lengths down to 6.9 ps. Moreover, Iliev *et al.* [154] demonstrated passive mode locking of a diode-pumped Nd:YVO_4 laser exploiting both NLM and CSM. The pulse repetition rate of the laser is 117 MHz with average power ranging from 0.5 to 3.1 W and pulse duration from 2.9 to 5.2 ps. The NLM ensures self-starting and self-sustaining mode locking, while the CSM process is the dominant pulse shortening mechanism that can generate pulse duration below 10 ps. The advantages of this hybrid technique lie in both the high average output power and the short pulsewidth down to several picoseconds. To date, most of the studies on intracavity SHG mode locking were focused on the 1.06 μm laser system, and more recently much attention has been paid to the development of 1.34 μm mode-locking lasers. Liu *et al.* [155] reported the first realization of an NLM mode-locked diode-pumped Nd:YVO_4 laser operating at 1342 nm with a PPLN crystal. The average output power is about ~1.5 W, and the pulsewidth and the repetition rate of the output laser are 9.5 ps and 101 MHZ, respectively. Almost at the same time,

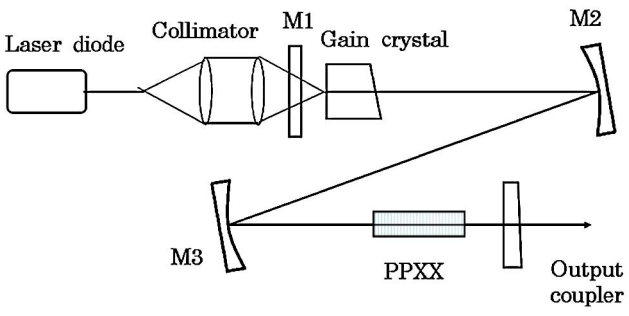

Fig. 17. Schematic experimental setup of passively mode-locking lasers with optical superlattice.

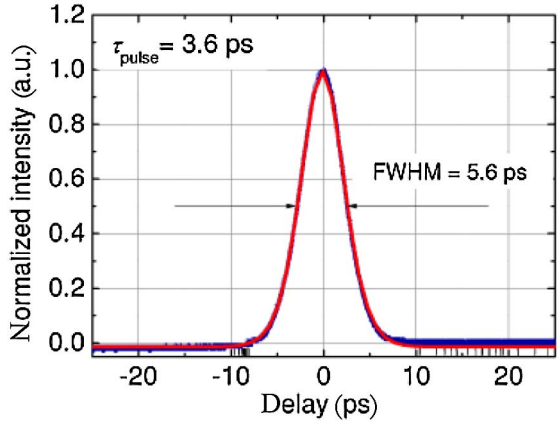

Fig. 18. Typical autocorrelation trace of passively mode-locked pulses with optical superlattice. Selected from Ref. [153].

Iliev *et al.* [155] demonstrated CSM of a 1.34 μm Nd:YVO_4 laser in MgO:PPSLT crystal. A high average power of about 1 W and a short pulse duration of 3.6 ps were simultaneously obtained from this passively mode-locked 1.34 μm diode-pumped laser source. Figure 18 shows a typical autocorrelation trace of passively mode-locked pulses with optical superlattice, which is selected from [156].

7. CONCLUSION AND OUTLOOK

To summarize, from the 1980s, the QPM-material fabrication techniques have been well developed, and among them, the electric-field poling technique and its variations are applied to the commonly used nonlinear optical materials, such as LN-family, LT-family, and KTP crystals. Domain periods of a few micrometers to several tens of micrometers are fabricated for visible and IR applications. A challenge still remained in the fabrication of submicrometer or nanoscale ferroelectric domains, which have current and future applications such as efficient first-order QPM UV SHG, electro-optic Bragg gratings with an unrivalled capacity of integration, counterpropagation optical parametric interactions, and enhanced second-order optical processes in nonlinear photonic crystals [157,158].

With the development of QPM theory, nonlinear optical materials, materials fabrication techniques, all-solid-state laser pumping sources, and novel optical cavity geometries, new laser light sources based on parametric processes can extend the spectral range from the UV to the mid-IR, with temporal coverage in all time scales from CW to ultrafast femtosecond.

Nowadays, the QPM technique has entered a new regime. On the one hand, the QPM-based all-solid-state laser technique has brought out practical applications in modern laser industries, while, on the other hand, the QPM technique has paved a new way for fundamental research in quantum optics [159]. From the early study of multipartite continuous-variable entanglement [160] to the recent studies in the transformation of spatial and temporal properties of entangled photons [161–166], the domain-engineered crystal has taken a key role in the engineering of new types of photonic entanglement. In particular, for those QPM crystals capable of ensuring multiple nonlinear processes, several functions can be integrated into a single crystal wafer and on-chip steering of entangled photons can be achieved, by which the QPM crystal is proved to be a promising candidate for the future integrated quantum information processing.

ACKNOWLEDGMENTS

This work was supported by the National Natural Science Foundation of China (Nos. 61205140, 11274165, and 11021403), the Jiangsu Science Foundation (BK2011545), the State Key Program for Basic Research of China (Nos. 2010CB630703 and 2011CBA00205), and the PAPD.

REFERENCES

1. T. H. Maiman, "Stimulated optical radiation in ruby," Nature **187**, 493–494 (1960).
2. P. A. Franken, A. E. Hill, C. W. Peters, and G. Weinreich, "Generation of optical harmonics," Phys. Rev. Lett. **7**, 118–119 (1961).
3. D. A. Kleinman, "Theory of second harmonic generation of light," Phys. Rev. **128**, 1761–1775 (1962).
4. J. A. Armstrong, N. Bloembergen, J. Ducuing, and P. S. Pershan, "Interactions between light waves in dielectric," Phys. Rev. **127**, 1918–1939 (1962).
5. M. S. Piltch, C. D. Cantrell, and R. C. Sze, "Infrared second-harmonic generation in nonbirefringent cadmium telluride," J. Appl. Phys. **47**, 3514–3517 (1976).
6. A. Szilagyi, A. Hordvik, and H. Schlossberg, "A quasi-phase-matching technique for efficient optical mixing and frequency doubling," J. Appl. Phys. **47**, 2025–2032 (1976).
7. D. E. Thompson, J. D. McMullen, and D. B. Anderson, "Second-harmonic generation in GaAs "stack of plates" using high-power CO2 laser radiation," Appl. Phys. Lett. **29**, 113–115 (1976).
8. M. Okada, K. Takizawa, and S. Ieiri, "Second harmonic generation by periodic laminar structure of nonlinear optical crystal," Opt. Commun. **18**, 331–334 (1976).
9. N. B. Ming, J. F. Hong, and D. Feng, "The growth striations and ferroelectric domain structures in Czochralski-grown $LiNbO_3$ single crystals," J. Mater. Sci. **17**, 1663–1670 (1982).
10. Y. L. Lu, Y. Q. Lu, X. F. Chen, G. P. Luo, C. C. Xue, and N. B. Ming, "Formation mechanism for ferroelectric domain structures in a $LiNbO_3$ optical superlattice," Appl. Phys. Lett. **68**, 2642–2644 (1996).
11. D. Feng, N. B. Ming, J. F. Hong, Y. S. Yang, J. S. Zhu, Z. Yang, and Y. N. Wang, "Enhancement of second-harmonic generation in $LiNbO_3$ crystals with periodic laminar ferroelectric domains," Appl. Phys. Lett. **37**, 607–609 (1980).
12. W. S. Wang, Q. Zou, Z. H. Geng, and D. Feng, "Study of $LiTaO_3$ crystals grown with a modulated structure I. Second harmonic generation in $LiTaO_3$ crystals with periodic laminar ferroelectric domains," J. Cryst. Growth **79**, 706–709 (1986).
13. M. M. Fejer, J. L. Nightingale, G. A. Magel, and R. L. Byer, "Laser-heated miniature pedestal growth apparatus for single-crystal optical fibers," Rev. Sci. Instrum. **55**, 1791–1796 (1984).
14. Y. S. Luh, R. S. Feigelson, M. M. Fejer, and R. Byer, "Ferroelectric domain structures in $LiNbO_3$ single-crystal fibers," J. Cryst. Growth **78**, 135–143 (1986).
15. G. A. Magel, M. M. Fejer, and R. L. Byer, "Quasi-phase-matched second-harmonic generation of blue light in periodically poled $LiNbO_3$," Appl. Phys. Lett. **56**, 108–110 (1990).
16. D. H. Jundt, G. A. Magel, M. M. Fejer, and R. L. Byer, "Periodically poled $LiNbO_3$ for high-efficiency second-harmonic generation," Appl. Phys. Lett. **59**, 2657–2659 (1991).
17. E. J. Lim, M. M. Fejer, and R. L. Byer, "Second-harmonic generation of green light in periodically-poled planar lithium niobate waveguide," Electron. Lett. **25**, 174–175 (1989).
18. E. J. Lim, M. M. Fejer, R. L. Byer, and W. J. Kozlovsky, "Blue light generation by frequency doubling in periodically poled lithium niobate channel waveguide," Electron. Lett. **25**, 731–732 (1989).
19. J. Webjörn, F. Laurell, and G. Arvidsson, "Blue light generated by frequency doubling of laser diode light in a lithium niobate channel waveguide," IEEE Photon. Technol. Lett. **1**, 316–318 (1989).
20. S. Miyazawa, "Ferroelectric domain inversion in Ti-diffused $LiNbO_3$ optical waveguide," J. Appl. Phys. **50**, 4599–4603 (1979).
21. J. D. Bierlein, D. B. Laubacher, J. B. Brown, and C. J. van der Poel, "Balanced phase matching in segmented $KTiOPO_4$ waveguides," Appl. Phys. Lett. **56**, 1725–1727 (1990).
22. C. J. van der Poel, J. D. Bierlein, J. B. Brown Co., and S. Colak, "Efficient type I blue second-harmonic generation in periodically segmented $KTiOPO_4$ waveguides," Appl. Phys. Lett. **57**, 2074–2076 (1990).
23. M. Yamada, N. Nada, M. Saitoh, and K. Watanabe, "First-order quasi-phase matched $LiNbO_3$ waveguide periodically poled by applying an external field for efficient blue second-harmonic generation," Appl. Phys. Lett. **62**, 435–436 (1993).
24. H. Ito, C. Takyu, and H. Inaba, "Fabrication of periodic domain grating in $LiNbO_3$ by electron beam writing for application of nonlinear optical processes," Electron. Lett. **27**, 1221–1222 (1991).

25. G. D. Miller, "Periodically poled lithium niobate: modeling, fabrication, and nonlinear-optical performance," Ph.D. thesis (Stanford University, 1998).
26. S. N. Zhu, Y. Y. Zhu, Z. Y. Zhang, H. Shu, H. F. Wang, J. F. Hong, C. Z. Ge, and N. B. Ming, "$LiTaO_3$ crystal periodically poled by applying an external pulsed field," J. Appl. Phys. **77**, 5481–5483 (1995).
27. W. P. Risk and S. D. Lau, "Periodic electric field poling of $KTiOPO_4$ using chemical patterning," Appl. Phys. Lett. **69**, 3999–4001 (1996).
28. Y. Y. Zhu, J. S. Fu, R. F. Xiao, and G. K. L. Wong, "Second harmonic generation in periodically domain-inverted $Sr_{0.6}Ba_{0.4}Nb_2O_6$ crystal plate," Appl. Phys. Lett. **70**, 1793–1795 (1997).
29. L. E. Myers, R. C. Eckardt, M. M. Fejer, R. L. Byer, W. R. Bosenberg, and J. W. Pierce, "Quasi-phase-matched optical parametric oscillators in bulk periodically poled $LiNbO_3$," J. Opt. Soc. Am. B **12**, 2102–2116 (1995).
30. L. E. Myers, "Quasi-phase-matched optical parametric oscillators in bulk periodically poled lithium niobate," Ph.D. thesis (Stanford University, 1995).
31. G. D. Miller, R. G. Batchko, M. M. Fejer, and R. L. Byer, "Visible quasi-phase-matched harmonic generation by electric-field-poled lithium niobate," Proc. SPIE **2700**, 34–35 (1996).
32. R. G. Batchko, V. Y. Shur, M. M. Fejer, and R. L. Boyd, "Backswitch poling in lithium niobate for high-fidelity domain patterning and efficient blue light generation," Appl. Phys. Lett. **75**, 1673–1675 (1999).
33. A. C. Busacca, C. L. Sones, V. Apostolopoulos, R. W. Eason, and S. Mailis, "Surface domain engineering in congruent lithium niobate single crystals: a route to submicron periodic poling," Appl. Phys. Lett. **81**, 4946–4948 (2002).
34. A. C. Busacca, C. L. Sones, R. W. Eason, and S. Mailis, "First-order quasi-phase-matched blue light generation in surface-poled Ti:indiffused lithium niobate waveguides," Appl. Phys. Lett. **84**, 4430–4432 (2004).
35. G. Zhong, J. Jian, and Z. Wu, "Measurement of optically induced refractive-index change of lithium niobate doped with different concentration of MgO," in *Proceedings of the 11th International Quantum Electronics Conference* (1980), pp. 631–635.
36. A. Kuroda, S. Kurimura, and Y. Uesu, "Domain inversion in ferroelectric MgO:$LiNbO_3$ by applying electric fields," Appl. Phys. Lett. **69**, 1565–1567 (1996).
37. S. Sonoda, I. Tsuruma, and M. Hatori, "Second harmonic generation in electric poled X-cut MgO-doped $LiNbO_3$ waveguides," Appl. Phys. Lett. **70**, 3078–3080 (1997).
38. T. Sugita, K. Mizuuchi, Y. Kitaoka, and K. Yamamoto, "Ultraviolet light generation in a periodically poled MgO:$LiNbO_3$ waveguide," Jpn. J. Appl. Phys. **40**, 1751–1753 (2001).
39. H. Ishizuki, I. Shoji, and T. Taira, "Periodical poling characteristics of congruent MgO:$LiNbO_3$ crystals at elevated temperature," Appl. Phys. Lett. **82**, 4062–4064 (2003).
40. H. Ishizuki, T. Taira, S. Kurimura, J. H. Ro, and M. Cha, "Periodic poling in 3-mm-thick MgO:$LiNbO_3$ crystals," Jpn. J. Appl. Phys. **42**, L108–L110 (2003).
41. H. Ishizuki and T. Taira, "High-energy quasi-phase-matched optical parametric oscillation in a periodically poled MgO:$LiNbO_3$ device with a 5 mm × 5 mm aperture," Opt. Lett. **30**, 2918–2920 (2005).
42. H. Ishizuki and T. Taira, "High energy quasi-phase matched optical parametric oscillation using Mg-doped congruent $LiTaO_3$ crystal," Opt. Express **18**, 253–258 (2010).
43. H. Ishizuki and T. Taira, "Half-joule output optical-parametric oscillation by using 10-mm-thick periodically poled Mg-doped congruent $LiNbO_3$," Opt. Express **20**, 20002–20010 (2012).
44. K. Mizuuchi, A. Morikawa, T. Sugita, and K. Yamamoto, "Efficient second-harmonic generation of 340-nm light in a 1.4-μm periodically poled bulk MgO:$LiNbO_3$," Jpn. J. Appl. Phys. **42**, L90–L91 (2003).
45. C. Y. J. Ying, A. C. Muir, C. E. Valdivia, H. Steigerwald, C. L. Sones, R. W. Eason, E. Soergel, and S. Mailis, "Light-mediated ferroelectric domain engineering and micro-structuring of lithium niobate crystals," Laser Photon. Rev. **6**, 526–548 (2012).
46. Q. Chen and W. P. Risk, "Periodic poling of $KTiOPO_4$ using an applied electric field," Electron. Lett. **30**, 1516–1517 (1994).
47. H. Karlsson and F. Laurell, "Electric field poling of flux grown $KTiOPO_4$," Appl. Phys. Lett. **71**, 3474–3476 (1997).
48. G. Rosenman, A. Skliar, D. Eger, M. Oron, and M. Katz, "Low temperature periodic electrical poling of flux-grown $KTiOPO_4$ and isomorphic crystals," Appl. Phys. Lett. **73**, 3650–3652 (1998).
49. C. Canalias, V. Pasiskevicius, and F. Laurell, "Periodic poling of $KTiOPO_4$: from micrometer to sub-micrometer domain gratings," Ferroelectrics **340**, 27–47 (2006).
50. C. Canalias, V. Pasiskevicius, R. Clemens, and F. Laurell, "Submicron periodically poled flux-grown $KTiOPO_4$," Appl. Phys. Lett. **82**, 4233–4235 (2003).
51. C. Canalias, V. Pasiskevicius, M. Fokine, and F. Laurell, "Backward quasi-phase-matched second-harmonic generation in submicrometer periodically poled flux-grown $KTiOPO_4$," Appl. Phys. Lett. **86**, 181105 (2005).
52. C. Canalias and V. Pasiskevicius, "Mirrorless optical parametric oscillator," Nat. Photonics **1**, 459–462 (2007).
53. L. A. Eyres, P. J. Tourreau, T. J. Pinguet, C. B. Ebert, J. S. Harris, M. M. Fejer, L. Becouarn, B. Gerard, and E. Lallier, "All-epitaxial fabrication of thick, orientation-patterned GaAs films for nonlinear optical frequency conversion," Appl. Phys. Lett. **79**, 904–906 (2001).
54. S. Kurimura, M. Harada, K. Muramatsu, M. Ueda, M. Adachi, T. Yamada, and T. Ueno, "Quartz revisits nonlinear optics: twinned crystal for quasi-phase matching," Opt. Mater. Express **1**, 1367–1375 (2011).
55. J. L. He, G. Z. Luo, H. T. Wang, S. N. Zhu, Y. Y. Zhu, Y. B. Chen, and N. B. Ming, "Generation of 840 mW of red light by frequency doubling a diode-pumped 1342 nm Nd:YVO_4 laser with periodically-poled $LiTaO_3$," Appl. Phys. B **74**, 537–539 (2002).
56. X. P. Hu, X. Wang, J. L. He, Y. X. Fan, S. N. Zhu, H. T. Wang, Y. Y. Zhu, and N. B. Ming, "Efficient generation of red light by frequency doubling in a periodically-poled nearly-stoichiometric $LiTaO_3$ crystal," Appl. Phys. Lett. **85**, 188–190 (2004).
57. X. P. Hu, X. Wang, Z. Yan, H. X. Li, J. L. He, and S. N. Zhu, "Generation of red light at 660 nm by frequency doubling a Nd:YAG laser with periodically-poled stoichiometric $LiTaO_3$," Appl. Phys. B **86**, 265–268 (2007).
58. R. Thompson, M. Tu, D. Aveline, N. Lundblad, and L. Maleki, "High power single frequency 780 nm laser source generated from frequency doubling of a seeded fiber amplifier in a cascade of PPLN crystals," Opt. Express **11**, 1709–1713 (2003).
59. S. Chiow, T. Kovachy, J. M. Hogan, and M. A. Kasevich, "Generation of 43 W of quasi-continuous 780 nm laser light via high-efficiency, single-pass frequency doubling in periodically poled lithium niobate crystals," Opt. Lett. **37**, 3861–3863 (2012).
60. D. L. Hart, L. Goldberg, and W. K. Burns, "Red light generation by sum frequency mixing of Er/Yb fibre amplifier output in QPM $LiNbO_3$," Electron. Lett. **35**, 52–53 (1999).
61. J. Boullet, L. Lavoute, A. Desfarges Berthelemot, V. Kermène, P. Roy, V. Couderc, B. Dussardier, and A.-M. Jurdyc, "Tunable red-light source by frequency mixing from dual band Er/Yb co-doped fiber laser," Opt. Express **14**, 3936–3941 (2006).
62. P. A. Champert, S. V. Popov, M. A. Solodyankin, and J. R. Taylor, "1.4-W red generation by frequency mixing of seeded Yb and Er fiber amplifiers," IEEE Photon. Technol. Lett. **14**, 1680–1682 (2002).
63. J. Melkonian, T. My, F. Bretenaker, and C. Drag, "High spectral purity and tunable operation of a continuous singly resonant optical parametric oscillator emitting in the red," Opt. Lett. **32**, 518–520 (2007).
64. W. R. Bosenberg, J. I. Alexander, L. E. Myers, and R. W. Wallace, "2.5-W, continuous-wave, 629-nm solid-state laser source," Opt. Lett. **23**, 207–209 (1998).
65. G. D. Miller, R. G. Batchko, W. M. Tulloch, D. R. Weise, M. M. Fejer, and R. L. Byer, "42%-efficient single-pass cw second-harmonic generation in periodically poled lithium niobate," Opt. Lett. **22**, 1834–1836 (1997).
66. N. Pavel, I. Shoji, T. Taira, K. Mizuuchi, A. Morikawa, T. Sugita, and K. Yamamoto, "Room-temperature, continuous-wave 1-W green power by single-pass frequency doubling in a bulk

periodically poled MgO:$LiNbO_3$ crystal," Opt. Lett. **29**, 830–832 (2004).
67. S. V. Tovstonog, S. Kurimura, and K. Kitamura, "High power continuous-wave green light generation by quasiphase matching in Mg stoichiometric lithium tantalite," Appl. Phys. Lett. **90**, 051115 (2007).
68. S. C. Kumar, G. K. Samanta, and M. Ebrahim-Zadeh, "High-power, single-frequency, continuous-wave second-harmonic-generation of ytterbium fiber laser in PPKTP and MgO:sPPLT," Opt. Express **17**, 13711–13726 (2009).
69. I. Ricciardi, M. Rosa, A. Rocco, P. Ferraro, and P. Natale, "Cavity-enhanced generation of 6 W cw second-harmonic power at 532 nm in periodically-poled MgO:$LiTaO_3$," Opt. Express **18**, 10985–10994 (2010).
70. S. C. Kumar, G. K. Samanta, K. Devi, and M. Ebrahim-Zadeh, "High-efficiency, multicrystal, single-pass, continuous-wave second harmonic generation," Opt. Express **19**, 11152–11169 (2011).
71. G. C. Bhar, U. Chatterjee, and P. Datta, "Enhancement of second harmonic generation by double-pass configuration in barium borate," Appl. Phys. B **51**, 317–319 (1990).
72. V. Pruneri, R. Koch, P. G. Kazansky, W. A. Clarkson, P. St, J. Russell, and D. C. Hanna, "49 mW of cw blue light generated by first-order quasi-phasematched frequency doubling of a diode-pumped 946-nm Nd:YAG laser," Opt. Lett. **20**, 2375–2377 (1995).
73. R. G. Batchko, M. M. Fejer, R. L. Byer, D. Woll, R. Wallenstein, V. Y. Shur, and L. Erman, "Continuous-wave quasi-phase-matched generation of 60 mW at 465 nm by single-pass frequency doubling of a laser diode in backswitch-poled lithium niobate," Opt. Lett. **24**, 1293–1295 (1999).
74. X. P. Hu, G. Zhao, C. Zhang, Z. D. Xie, J. L. He, and S. N. Zhu, "High-power, blue-light generation in a dual-structure, periodically poled, stoichiometric $LiTaO_3$ crystal," Appl. Phys. B **87**, 91–94 (2007).
75. D. Woll, J. Schumacher, A. Robertson, M. A. Tremont, R. Wallenstein, M. Katz, D. Eger, and A. Englander, "250 mW of coherent blue 460-nm light generated by single-pass frequency doubling of the output of a mode-locked high-power diode laser in periodically poled KTP," Opt. Lett. **27**, 1055–1057 (2002).
76. P. Xu, K. Li, G. Zhao, S. N. Zhu, Y. Du, S. H. Ji, Y. Y. Zhu, N. B. Ming, L. Luo, K. F. Li, and K. W. Cheah, "Quasi-phase-matched generation of tunable blue light in a quasi-periodic structure," Opt. Lett. **29**, 95–97 (2004).
77. G. K. Samanta and M. Ebrahim-Zadeh, "Continuous-wave, single-frequency, solid-state blue source for the 425–489 nm spectral range," Opt. Lett. **33**, 1228–1230 (2008).
78. C.-M. Lai, I.-N. Hu, Y.-Y. Lai, Z.-X. Huang, L.-H. Peng, A. Boudrioua, and A.-H. Kung, "Upconversion blue laser by intracavity frequency self-doubling of periodically poled lithium tantalate parametric oscillator," Opt. Lett. **35**, 160–162 (2010).
79. J. Zimmermann, J. Struckmeier, M. R. Hofmann, and J. Meyn, "Tunable blue laser based on intracavity frequency doubling with a fan-structured periodically poled $LiTaO_3$ crystal," Opt. Lett. **27**, 604–606 (2002).
80. J. D. Vance, C. Y. She, and H. Moosmüller, "Continuous-wave, all-solid-state, single-frequency 400-mW source at 589 nm based on doubly resonant sum-frequency mixing in a monolithic lithium niobate resonator," Appl. Opt. **37**, 4891–4896 (1998).
81. J. Yue, C.-Y. She, B. P. Williams, J. D. Vance, P. E. Acott, and T. D. Kawahara, "Continuous-wave sodium D_2 resonance radiation generated in single-pass sum-frequency generation with periodically poled lithium niobate," Opt. Lett. **34**, 1093–1095 (2009).
82. A. J. Tracy, C. Lopez, A. Hankla, D. J. Bamford, D. J. Cook, and S. J. Sharpe, "Generation of high-average-power visible light in periodically poled nearly stoichiometric lithium tantalite," Appl. Opt. **48**, 964–968 (2009).
83. E. Mimoun, L. Sarlo, J. Zondy, J. Dalibard, and F. Gerbier, "Sum-frequency generation of 589 nm light with near-unit efficiency," Opt. Express **16**, 18684–18691 (2008).
84. L. N. Zhao, J. Su, X. P. Hu, X. J. Lv, Z. D. Xie, G. Zhao, P. Xu, and S. N. Zhu, "Single-pass sum-frequency-generation of 589-nm yellow light based on dual-wavelength Nd:YAG laser with periodically-poled $LiTaO_3$ crystal," Opt. Express **18**, 13331–13336 (2010).
85. Y. F. Chen, S. W. Tsai, S. C. Wang, Y. C. Huang, T. C. Lin, and B. C. Wong, "Efficient generation of continuous-wave yellow light by single-pass sum-frequency mixing of a diode-pumped Nd:YVO_4 dual-wavelength laser with periodically poled lithium niobate," Opt. Lett. **27**, 1809–1811 (2002).
86. Y. F. Chen, "Cw dual-wavelength operation of a diode-end-pumped Nd:YVO_4 laser," Appl. Phys. B. **70**, 475–478 (2000).
87. D. Georgiev, V. P. Gapontsev, A. G. Dronov, M. Y. Vyatkin, A. B. Rulkov, S. V. Popov, and J. R. Taylor, "Watts-level frequency doubling of a narrow line linearly polarized Raman fiber laser to 589 nm," Opt. Express **13**, 6772–6776 (2005).
88. Y. Yuan, L. Zhang, Y. H. Liu, X. J. Lu, G. Zhao, Y. Feng, and S. N. Zhu, "Sodium guide star laser generation by single-pass frequency doubling in a periodically poled near-stoichiometric $LiTaO_3$ crystal," Sci. China Ser. B **56**, 125–128 (2013).
89. R. T. White, I. T. McKinnie, S. D. Butterworth, G. W. Baxter, D. M. Warrington, P. G. R. Smith, G. W. Ross, and D. C. Hanna, "Tunable single-frequency ultraviolet generation from a continuous-wave Ti:sapphire laser with an intracavity PPLN frequency doubler," Appl. Phys. B **77**, 547–550 (2003).
90. K. Mizuuchi, T. Sugita, and K. Yamamoto, "Generation of 360-nm ultraviolet light in first-order periodically poled bulk MgO:$LiNbO_3$," Opt. Lett. **28**, 935–937 (2003).
91. J.-P. Meyn and M. M. Fejer, "Tunable ultraviolet radiation by second-harmonic generation in periodically poled lithium tantalite," Opt. Lett. **22**, 1214–1216 (1997).
92. K. Mizuuchi and K. Yamamoto, "Generation of 340-nm light by frequency doubling of a laser diode in bulk periodically poled $LiTaO_3$," Opt. Lett. **21**, 107–109 (1996).
93. P. A. Champert, S. V. Popov, J. R. Taylor, and J. P. Meyn, "Efficient second-harmonic generation at 384 nm in periodically poled lithium tantalate by use of a visible Yb-Er-seeded fiber source," Opt. Lett. **25**, 1252–1254 (2000).
94. Z. W. Liu, S. N. Zhu, Y. Y. Zhu, Y. Q. Qin, J. L. He, C. Zhang, H. T. Wang, N. B. Ming, X. Y. Liang, and Z. Y. Xu, "Quasi-Cw ultraviolet generation in a dual-periodic $LiTaO_3$ superlattice by frequency tripling," Jpn. J. Appl. Phys. **40**, 6841–6844 (2001).
95. S. Wang, V. Pasiskevicius, J. Hellstrã, F. Laurell, and H. Karlsson, "First-order type II quasi-phase-matched UV generation in periodically poled KTP," Opt. Lett. **24**, 978–980 (1999).
96. S. Wang, V. Pasiskevicius, F. Laurell, and H. Karlsson, "Ultraviolet generation by first-order frequency doubling in periodically poled $KTiOPO_4$," Opt. Lett. **23**, 1883–1885 (1998).
97. B. Zhang, Y. J. Ding, and I. B. Zotova, "Efficient ultrafast ultraviolet generation based on frequency doubling in short-period periodically-poled $KTiOPO_4$ crystal," Appl. Phys. B **99**, 629–632 (2010).
98. E. G. Víllora, K. Shimamura, K. Sumiya, and H. Ishibashi, "Birefringent and quasi phase-matching with BaMgF4for vacuum-UV/UV and mid-IR all solid-state lasers," Opt. Express **17**, 12362–12378 (2009).
99. D. Shechtman, I. Blech, D. Gratias, and J. W. Cahn, "Metallic phase with long-range orientational order and no translational symmetry," Phys. Rev. Lett. **53**, 1951–1953 (1984).
100. J. Feng, Y. Y. Zhu, and N. B. Ming, "Harmonic generation in an optical Fibonacci superlattice," Phys. Rev. B **41**, 5578–5582 (1990).
101. B. Y. Gu, B. Z. Dong, Y. Zhang, and G. Z. Yang, "Enhanced harmonic generation in aperiodic optical superlattice," Appl. Phys. Lett. **75**, 2175–2177 (1999).
102. H. Liu, S. N. Zhu, Y. Y. Zhu, N. B. Ming, X. C. Lin, W. J. Ling, A. Y. Yao, and Z. Y. Xu, "Multiple-wavelength second-harmonic generation in aperiodic optical superlattices," Appl. Phys. Lett. **81**, 3326–3328 (2002).
103. M. H. Chou, K. R. Parameswaran, and M. M. Fejer, "Multiple-channel wavelength conversion by use of engineered quasi-phase-matching structure in $LiNbO_3$ waveguides," Opt. Lett. **24**, 1157–1159 (1999).
104. V. Berger, "Nonlinear photonic crystals," Phys. Rev. Lett. **81**, 4136–4139 (1998).
105. B. Q. Ma, T. Wang, Y. Sheng, P. G. Ni, Y. Q. Wang, B. Y. Cheng, and D. Z. Zhang, "Quasiphase matched harmonic generation in

a two-dimensional octagonal photonics superlattice," Appl. Phys. Lett. **87**, 251103 (2005).
106. L. H. Peng, C. C. Hsu, and Y. C. Shih, "Second-harmonic green generation from two-dimensional x(2) nonlinear photonic crystal with orthorhombic lattice structure," Appl. Phys. Lett. **83**, 3447–3449 (2003).
107. R. K. P. Zia and W. J. Dallas, "A simple derivation of quasi-crystalline spectra," J. Phys. A **18**, L341–L345 (1985).
108. S. N. Zhu, Y. Y. Zhu, and N. B. Ming, "Quasi-phase-matched third-harmonic generation in a quasi-periodic optical superlattice," Science **278**, 843–846 (1997).
109. K. Yamamoto, H. Yamamoto, and T. Taniuchi, "Simultaneous sum-frequency and second-harmonic generation from a proton-exchanged MgO-doped $LiNbO_3$ waveguide," Appl. Phys. Lett. **58**, 1227–1229 (1991).
110. F. Laurell, J. B. Brown, and J. D. Bierlein, "Simultaneous generation of UV and visible light in segmented KTP waveguides," Appl. Phys. Lett. **62**, 1872–1874 (1993).
111. M. L. Sundheimer, A. Villeneuve, G. I. Stegeman, and J. D. Bierlein, "Simultaneous generation of red, green and blue light in a segmented KTP waveguide using a single source," Electron. Lett. **30**, 975–976 (1994).
112. P. Baldi, C. G. Trevino-Palacios, G. I. Stegeman, M. P. De Micheli, D. B. Ostrowsky, D. Delacourt, and M. Papuchon, "Simultaneous generation of red, green and blue light in room temperature periodically poled lithium niobate waveguides using single source," Electron. Lett. **31**, 1350–1351 (1995).
113. E. Cantelar, G. A. Torchia, J. A. Sanz-García, P. L. Pernas, G. Lifante, and F. Cusso, "Red, green, and blue simultaneous generation in aperiodically poled Zn-diffused $LiNbO_3$:Er^{3+}/Yb^{3+} nonlinear channel waveguides," Appl. Phys. Lett. **83**, 2991–2993 (2003).
114. D. Jaque, J. Capmany, and J. G. Sole, "Red, green, and blue laser light from a single Nd:$YAl_3(BO_3)_4$ crystal based on laser oscillation at 1.3 μm," Appl. Phys. Lett. **75**, 325–327 (1999).
115. J. J. Romero, D. Jaque, J. F. Sole, and A. A. Kaminskii, "Simultaneous generation of coherent light in the three fundamental colors by quasicylindrical ferroelectric domains in $Sr_{0.6}Ba_{0.4}(NbO_3)_2$," Appl. Phys. Lett. **81**, 4106–4108 (2002).
116. J. Capmany, "Simultaneous generation of red, green, and blue continuous-wave laser radiation in Nd^{3+}-doped aperiodically poled lithium niobate," Appl. Phys. Lett. **78**, 144–146 (2001).
117. J. L. He, J. Liao, H. Liu, J. Du, F. Xu, H. T. Wang, S. N. Zhu, Y. Y. Zhu, and N. B. Ming, "Simultaneous cw red, yellow, and green light generation, "traffic signal lights," by frequency doubling and sum-frequency mixing in an aperiodically poled $LiTaO_3$," Appl. Phys. Lett. **83**, 228–230 (2003).
118. J. Liao, J. L. He, H. Liu, H. T. Wang, S. N. Zhu, Y. Y. Zhu, and N. B. Ming, "Simultaneous generation of red, green, and blue quasi-continuous-wave coherent radiation based on multiple quasi-phase-matched interactions from a single, aperiodically-poled $LiTaO_3$," Appl. Phys. Lett. **82**, 3159–3161 (2003).
119. H. X. Li, Y. X. Fan, P. Xu, S. N. Zhu, P. Lu, Z. D. Gao, H. T. Wang, Y. Y. Zhu, N. B. Ming, and J. L. He, "530-mW quasi-white-light generation using all-solid-state laser technique," J. Appl. Phys. **96**, 7756–7758 (2004).
120. X. P. Hu, G. Zhao, Z. Yan, X. Wang, Z. D. Gao, H. Liu, J. L. He, and S. N. Zhu, "High-power red-green-blue laser light source based on intermittent oscillating dual-wavelength Nd:YAG laser with a cascaded $LiTaO_3$ superlattice," Opt. Lett. **33**, 408–410 (2008).
121. X. W. Fan, J. L. He, H. T. Huang, and L. Xue, "An intermittent oscillation dual-wavelength diode-pumped Nd:YAG laser," IEEE J. Quantum Electron. **43**, 884–888 (2007).
122. B. Henrich, T. Herrmann, J. Kleilbauer, R. Knappe, A. Nebel, and R. Wallenstein, "Concepts and technologies of advanced RGB sources," in *Advanced Solid-State Lasers Conference* (2002), pp. 179–181.
123. Z. W. Liu, S. N. Zhu, Y. Y. Zhu, H. Liu, Y. Q. Lu, H. T. Wang, N. B. Ming, X. Y. Liang, and Z. Y. Xu, "A scheme to realize three-fundamental-colors laser based on quasi-phase matching," Solid State Commun. **119**, 363–366 (2001).
124. Z. D. Gao, S. N. Zhu, S. Y. Tu, and A. H. Kung, "Monolithic red-green-blue laser light source based on cascaded wavelength conversion in periodically poled stoichiometric lithium tantalite," Appl. Phys. Lett. **89**, 181101 (2006).
125. P. Xu, L. N. Zhao, X. J. Lv, J. Lu, Y. Yuan, G. Zhao, and S. N. Zhu, "Compact high-power red-green-blue laser light source generation from a single lithium tantalate with cascaded domain modulation," Opt. Express **17**, 9509–9514 (2009).
126. S. T. Lin, Y. Y. Lin, R. Y. Tu, T. D. Wang, and Y. C. Huang, "Fiber-laser-pumped CW OPO for red, green, blue laser generation," Opt. Express **18**, 2361–2367 (2010).
127. R. S. Cudney, M. Robles-Agudo, and L. A. Rois, "RGB source based on simultaneous quasi-phasematched second and third harmonic generation in periodically poled lithium niobate," Opt. Express **14**, 10663–10668 (2006).
128. P. Xu, Z. D. Xie, H. Y. Leng, J. S. Zhao, J. F. Wang, X. Q. Yu, Y. Q. Qin, and S. N. Zhu, "Frequency self-doubling optical parametric amplification: noncollinear red–green–blue light-source generation based on a hexagonally poled lithium tantalite," Opt. Lett. **33**, 2791–2793 (2008).
129. L. N. Zhao, Z. Qi, Y. Yuan, J. Lu, Y. H. Liu, C. D. Chen, X. J. Lv, Z. D. Xie, X. P. Hu, G. Zhao, P. Xu, and S. N. Zhu, "Integrated noncollinear red–green–blue laser light source using a two-dimensional nonlinear photonic quasicrystal," J. Opt. Soc. Am. B **28**, 608–612 (2011).
130. L. E. Myers, G. D. Miller, R. C. Eckardt, M. M. Fejer, R. L. Byer, and W. R. Bosenberg, "Quasi-phase-matched 1.064-μm-pumped optical parametric oscillator in bulk periodically poled $LiNbO_3$," Opt. Lett. **20**, 52–54 (1995).
131. M. L. Bortz, M. A. Arbore, and M. M. Fejer, "Quasi-phase-matched optical parametric amplification and oscillation in periodically poled $LiNbO_3$ waveguides," Opt. Lett. **20**, 49–51 (1995).
132. A. Zukauskas, N. Thilmann, V. Pasiskevicius, F. Laurell, and C. Canalias, "5 mm thick periodically poled Rb-doped KTP for high energy optical parametric frequency conversion," Opt. Mater. Express **1**, 201–206 (2011).
133. V. Pruneri, S. D. Butterworth, and D. C. Hanna, "Low-threshold picosecond optical parametric oscillation in quasi-phase-matched lithium niobate," Appl. Phys. Lett. **69**, 1029–1031 (1996).
134. A. Galvanauskas, M. A. Arbore, M. M. Fejer, M. E. Fermann, and D. Harter, "Fiber-laser-based femtosecond parametric generator in bulk periodically poled $LiNbO_3$," Opt. Lett. **22**, 105–107 (1997).
135. S. D. Butterworth, P. G. R. Smith, and D. C. Hanna, "Picosecond Ti:sapphire-pumped optical parametric oscillator based on periodically poled $LiNbO_3$," Opt. Lett. **22**, 618–620 (1997).
136. S. Chaitanya Kumar and M. Ebrahim-Zadeh, "High-power, fiber-laser-pumped, picosecond optical parametric oscillator based on MgO:sPPLT," Opt. Express **19**, 26660–26665 (2011).
137. C. W. Hoyt, M. Sheik-Bahae, and M. Ebrahim-Zadeh, "High-power picosecond optical parametric oscillator based on periodically poled lithium niobate," Opt. Lett. **27**, 1543–1545 (2002).
138. M. V. O'Connor, M. A. Watson, D. P. hepherd, D. C. Hanna, J. H. V. Price, A. Malinowski, J. Nilsson, N. G. R. Broderick, D. J. Richardson, and L. Lefort, "Synchronously pumped optical parametric oscillator driven by a femtosecond mode-locked fiber laser," Opt. Lett. **27**, 1052–1054(2002).
139. T. Sudmeyer, J. Aus der Au, R. Paschotta, U. Keller, P. G. R. Smith, G. W. Ross, and D. C. Hanna, "Femtosecond fiber-feedback optical parametric osicalltor," Opt. Lett. **26**, 304–306 (2001).
140. N. Coluccelli, H. Fonnum, M. Haakestad, A. Gambetta, D. Gatti, M. Marangoni, P. Laporta, and G. Galzerano, "25-MHz synchronously pumped optical parametric oscillator at 2.25-2.6 um and 4.1-4.9 μm," Opt. Express **20**, 22042–22047 (2012).
141. L. E. Myers, W. R. Bosenberg, J. I. Alexander, M. A. Arbore, M. M. Fejer, and R. L. Byer, "CW singly resonant optical parametric oscillators based on 1.064-um pumped periodically poled $LiNbO_3$," in *Proceedings on Advanced Solid State Lasers*, S. A. Payne and C. R. Pollock, eds. (1996), p. 35–37.
142. S. C. Kumar, R. Das, G. K. Samanta, and M. Ebrahim-Zadeh, "Optimally-output-coupled, 17.5 W, fiber-laser-pumped continuous-wave optical parametric oscillator," Appl. Phys. B. **102**, 31–35 (2011).

143. R. Sowade, I. Breunig, J. Kiessling, and K. Buse, "Influence of the pump threshold on the single-frequency output power of singly resonant optical parametric oscillators," Appl. Phys. B. **96**, 25–28 (2009).
144. R. Das, S. C. Kumar, G. K. Samanta, and M. Ebrahim-Zadeh, "Broadband, high-power, continuous-wave, mid-infrared source using extended phase-matching bandwidth in MgO: PPLN," Opt. Lett. **34**, 3836–3838 (2009).
145. U. Strossner, J. P. Meyn, R. Wallenstein, P. Urenski, A. Arie, G. Roseman, J. Mlynek, S. Schiller, and A. Peters, "Single-frequency continuous-wave optical parametric oscillator system with an ultrawide tuning range of 550 to 2830 nm," J. Opt. Soc. Am. B **19**, 1419–1424 (2002).
146. T. Petelski, R. S. Conroy, K. Bencheikh, J. Mlynek, and S. Schiller, "All-soild-state, tunable, single-frequency source of yellow light for high-resolution spectroscopy," Opt. Lett. **26**, 1013–1015 (2001).
147. J. R. Schwesyg, C. R. Phillips, K. Ioakeimidi, M. C. C. Kajiyama, M. Falk, D. H. Jundt, K. Buse, and M. M. Fejer, "Suppression of mid-infrared light absorption in undoped congruent lithium niobate crystals," Opt. Lett. **35**, 1070–1072 (2010).
148. K. A. Stankov and J. Jethwa, "A new mode-locking technique using a nonlinear mirror," Opt. Commun. **66**, 41–46 (1988).
149. G. Cerullo, S. De Silvestri, A. Monguzzi, D. Segaka, and V. Magni, "Self-starting mode-locking of a CW Nd:YAG laser using cascaded second-order nonlinearities," Opt. Lett. **20**, 746–748 (1995).
150. Y. F. Chen, S. W. Tsai, and S. C. Wang, "High-power diode-pumped nonlinear mirror mode-locked Nd:YVO_4 laser with periocailly-poled KTP," Appl. Phys. B **72**, 395–397 (2001).
151. S. J. Holmgren, V. Pasiskevicius, and F. Laurell, "Generation of 2.8 ps pulses by mode-locking a Nd:GdVO4 laser with defocusing cascaded Kerr lensing in periodically poled KTP," Opt. Express **13**, 5270–5278 (2005).
152. H. Iliev, I. Buchvarov, S. Kurimura, and V. Petrov, "High-power picosecond Nd:GdVO4 laser mode locked by SHG in periodically poled stoichiometric lithium tantalite," Opt. Lett. **35**, 1016–1018 (2010).
153. S. J. Holmgren, A. Fragemann, V. Pasiskevicius, and F. Laurell, "Active and passive hybrid mode-locking of a Nd:YVO_4 laser with a single partially poled KTP crystal," Opt. Express **14**, 6675–6680 (2006).
154. H. Iliev, D. Chuchumishev, I. Buchvarov, and V. Petrov, "Passive mode-locking of a diode-pumped Nd:YVO_4 laser by intracavity SHG in PPKTP," Opt. Express **18**, 5754–5762 (2010).
155. Y. H. Liu, Z. D. Xie, S. D. Pan, X. J. Lv, Y. Yuan, X. P. Hu, J. Lu, L. N. Zhao, C. D. Chen, G. Zhao, and S. N. Zhu, "Diode-pumped passively mode-locked Nd:YVO_4 laser at 1342 nm with periodically poled $LiTaO_3$," Opt. Lett. **36**, 698–700 (2011).
156. H. Iliev, I. Buchvarov, S. Kurimura, and V. Petrov, "1.34-μm Nd:YVO_4 laser mode-locked by SHG-lens formation in periodically-poled stoichiometric lithium tantalite," Opt. Express **19**, 21754–21759 (2011).
157. V. Y. Shur, "Domain nanotechnology in ferroelectric single crystals: lithium niobate and lithium tantalate family," Ferroelectrics **443**, 71–82 (2013).
158. J. J. Li, Z. Y. Li, and D. Z. Zhang, "Second harmonic generation in one-dimensional nonlinear photonic crystals solved by the transfer matrix method," Phys. Rev. E **75**, 056606 (2007).
159. P. Xu and S. N. Zhu, "Quasi-phase-matching engineering of entangled photons," AIP Adv. **2**, 041401 (2012).
160. Y. B. Yu, Z. D. Xie, X. Q. Yu, H. X. Li, P. Xu, H. M. Yao, and S. N. Zhu, "Generation of three-mode continuous-variable entanglement by cascaded nonlinear interactions in a quasiperiodic superlattice," Phys. Rev. A **74**, 042332 (2006).
161. X. Q. Yu, P. Xu, Z. D. Xie, J. F. Wang, H. Y. Leng, J. S. Zhao, S. N. Zhu, and N. B. Ming, "Transforming spatial entanglement using a domain-engineering technique," Phys. Rev. Lett. **101**, 233601 (2008).
162. H. Y. Leng, X. Q. Yu, Y. X. Gong, P. Xu, Z. D. Xie, H. Jin, C. Zhang, and S. N. Zhu, "On-chip steering of entangled photons in nonlinear photonic crystals," Nat. Commun. **2**, 429 (2011).
163. P. Xu, H. Y. Leng, Z. H. Zhu, Y. F. Bai, H. Jin, Y. X. Gong, X. Q. Yu, Z. D. Xie, S. Y. Mu, and S. N. Zhu, "Lensless imaging by entangled photons from quadratic nonlinear photonic crystals," Phys. Rev. A **86**, 013805 (2012).
164. H. Jin, P. Xu, J. S. Zhao, H. Y. Leng, M. L. Zhong, and S. N. Zhu, "Observation of quantum Talbot effect from a domain-engineered nonlinear photonic crystal," Appl. Phys. Lett. **101**, 211115 (2012).
165. Y. F. Bai, P. Xu, Z. D. Xie, Y. X. Gong, and S. N. Zhu, "Mode-locked biphoton generation by concurrent quasi-phase-matching," Phys. Rev. A **85**, 053807 (2012).
166. S. E. Harris, "Chirp and compress: toward single-cycle biphotons," Phys. Rev. Lett. **98**, 063602 (2007).